NORWEGIAN SCHOOL OF SPORT SCIENCES

Ola Røkke

Validation of force-, velocity-, and acceleration-time curves and temporal characteristics as output data from the 1080 Sprint

Master thesis in Sport Sciences
Department of Physical Performance
Norwegian School of Sport Sciences, 2018

Abstract

Background: Temporal characteristics and mechanical profiling are two methods that provide a step by step and overall description of running. Recently, a testing and training system (1080 Sprint, Lindingö, Sweden), which not only measures time and distance, but also force, while providing resistance or assistance during running and sprinting became commercially available. This device allows coaches, clinicians and researchers to implement resisted and assisted running in training, rehabilitation and research projects whilst obtaining different physical profiles using only one piece of equipment. The data obtained show a cyclical behavior which can be contributed to individual step mechanics and can be used to study the temporal characteristics of resisted and assisted sprint running. Step, flight and cycle distance as well as other relevant time parameters can be determined. This thesis investigated the validity of measuring temporal characteristics with the system mentioned above.

Methods: Eight subjects (Age: 26 ± 2 years, height: 178 ± 9 cm, weight: 78 ± 10 kg) completed two test days each consisting of 10, 30 m runs with increasing different resistances (1, 3, 6, 9 and 12 kg). The 1080 Sprint provided the resistance and the measurements of time, distance, velocity and force at a sample rate of 333 Hz. Simultaneously, force sensitive resistors (FSR) sensors placed under the insole of each foot were used as criterion for the measurement of contact time.

Results: It was not possible to estimate contact time with the 1080 Sprint, but step time data was successfully estimated. Step time increased as load increased. Compared to FSR sensor data, 1080 Sprint systematically overestimated step time by 2.05 ± 1.08 ms, with a random error of 30.09 ± 4.28 ms.

Conclusion: Our results showed a systematic overestimation of ST of 2.05 ms in the 1080 Sprint when compared to FSR results. The determination of contact times was considered to be unreliable and should therefore not be used.

Table of contents

Acknowledgement

I would like to thank my supervisor Prof. Jan Cabri. Your knowledge and attention to detail has been of great importance during my work on this thesis.

Secondly, I would like to thank my co- supervisor Ola Eriksrud for discussion and practical insight during the data collection and feedback during the writing of this thesis.

Thank you to Øyvind Gløersen for immensely valuable technical and practical insights throughout the whole process.

To all subjects: Thank you for taking the time to participate in the study. I am grateful for your efforts.

Finally, I would like to thank my classmates, especially Thomas, Marius, Malin and Emelie, for professional discussion and social moments.

Ola Røkke

Oslo, October 2018

1. Introduction

Sprint running characteristics can be determined by different methods available on the market. Temporal characteristics and mechanical profiling are two methods that provide a step by step and overall description respectively. These have been available for field application using e.g. photocells, videography or laser technology. Recently, a testing and training system (1080 Sprint, Lidingö, Sweden) became available which not only measures time and distance, but also force, while providing resistance and/or assistance during running and sprinting. This allows coaches, clinicians and researchers to easily implement resisted and assisted running in training, rehabilitation and research projects whilst obtaining different physical profiles using only one piece of equipment. In addition, actual pulling force with the associated speed development is measured. The data obtained show a cyclical behavior which can be contributed to individual step mechanics and can be used to study the temporal characteristics of resisted and assisted sprint running. Step, flight and cycle distance as well as other time parameters can be determined. This information can be used to study amongst other variables, limb asymmetries, responses to loaded conditions, horizontal force impulse, leg and vertical stiffness (Morin, Dalleau, Kyröläinen, Jeannin, & Belli, 2005; Morin et al., 2015). However, this requires additional equipment beyond timing systems to obtain the temporal data. Foot switches, infrared light systems and different types of kinetic systems such as instrumented treadmills, force plates and pressure shoe soles are used for these purposes. The force-velocity (F-v), power-velocity (P-v) and load-velocity (L-v) profiling is gaining popularity among coaches and trainers all over the world, especially in track and field and team sports. How these profiles and also temporal characteristics with derived characteristics (impulse and stiffness) interact and contribute to performance, injury prevention and return to play strategies at different loads is not well understood. By implementing devices using robotic technology, the development of concepts of resisted/assisted training while studying the interaction of the temporal characteristics, impulses, asymmetries, stiffness and performance of sprinting, thus contributing to injury prevention and the decision to return to play, becomes possible.

2. Purpose and hypothesis

The aim of this study was to validate the temporal characteristics from the oscillations in the horizontal velocity-, acceleration- or force-time curves obtained from the 1080 Sprint, by comparing the results with simultaneously recorded (criterion) data from force sensitive resistors (FSR) located under the shoe soles.

We hypothesized that the onset of stance and flight phase occur at the onset of positive and negative horizontal acceleration respectively. We hypothesized that acceleration data are most accurate to determine the first (toe on) and last (toe off) point of foot contact, based on the positive and negative slopes of the acceleration-time curves.

3. Theory

Horizontal velocity-time and velocity-distance curves obtained from any sprint distance have an oscillatory nature based on horizontal force impulses. These oscillations are also observed in the acceleration-, force- and power-time curves. When analyzing such curves, the instances of foot contact and toe off are unknown. These oscillations provide an opportunity to explore if flight time (t_f) and contact time (t_c) can be defined, with the advantage of exploring variables and their possibilities described in chapter 3.3.

3.1 Sprinting temporal characteristics

Sprinting temporal characteristics describe how the athlete interacts with the ground. This can be objectified as step length (SL) and step time (ST), cycle length and cycle time, number of steps and sprint cycle frequency (Cronin et al., 2008). Step time can be further divided into contact time (t_c) and flight time (t_f). Furthermore, the product of step length and step frequency is defined as sprinting speed (Delecluse, 1998; Mann & Herman, 1985). Step length is defined as the length from the first point of contact of one foot, to the first point of contact for the other foot. Step time is the time it takes from the first point of contact to the first point of contact for the other foot. Cycle length is the distance from one foots first point of ground contact to the next point of ground contact for the same foot. Cycle time is the time it takes from one foot first is in contact with the ground, to the next time the same foot is in contact with the ground. In this thesis, "step" refers to half a running cycle (from foot contact to next contact of opposite foot), while "cycle" refers to a whole running cycle (from foot contact to next contact of the same foot) (Hunter, Marshall, & McNair, 2004). Many studies have shown that temporal characteristics affect sprinting velocity. For instance, a decrease in contact time and increasing step frequency, step length and flight time are strategies implemented to increase velocity (Figure 1) (Brughelli, Cronin, & Chaouachi, 2011; Rabita et al., 2015). During resisted sprinting, the decrease in contact time is not as low as for regular sprinting, while the increase in step frequency, step length and flight time is not as high as it is for non-resisted sprints (Cronin et al., 2008).

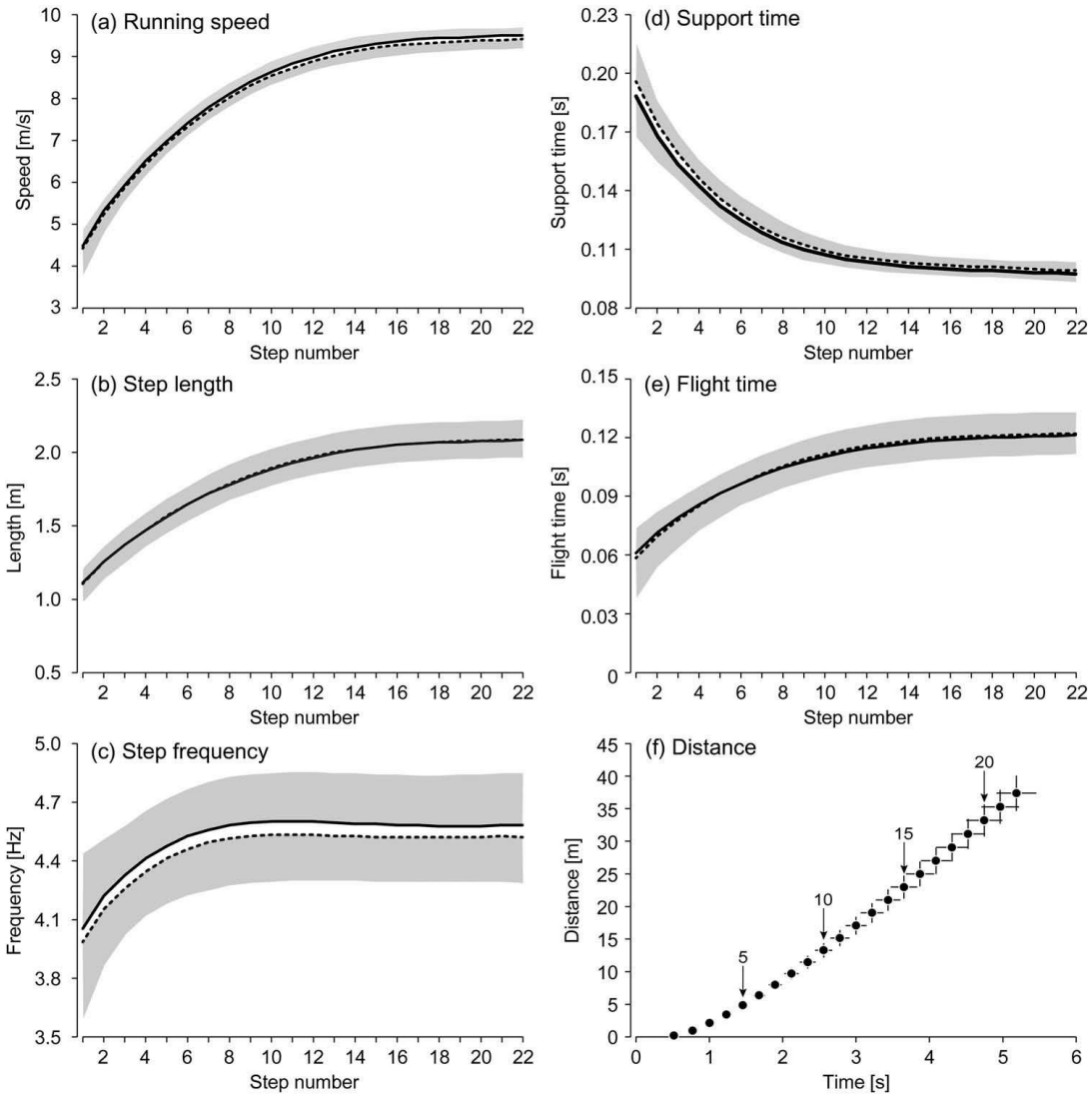

Figure 1: Mean and standard deviation of approximated running speed (a), step length (b), step frequency (c), support time (contact time) (d), flight time (e), and distance (f) with photocells (running speed) and force plates (step length, step frequency, support time, flight time and distance). Solid lines and dotted lines represent the fastest and slowest trials, respectively, except for distance. The grey shaded area represents standard deviation for each of the fastest and slowest trials. Mean distance from the starting line for the fastest trial is plotted against the mean time at each step (Nagahara, Mizutani, Matsuo, Kanehisa, & Fukunaga, 2018).

There are different ways to measure temporal characteristics (i.e. t_c and t_f). Most commonly used methods are force plates, instrumented treadmills, optical motion capture systems and infrared equipped mats (Bushnell & Hunter, 2007; Debaere, Jonkers, & Delecluse, 2013; Di Michele & Merni, 2014; Morin, Samozino, Zameziati, & Belli, 2007; Viitasalo et al., 1997). However, such systems are expensive, require technological support and are often only used in a laboratory settings, because of the sensitivity of the devices and the need for standardization (Ammann, Taube, & Wyss,

2016). Furthermore, the area of measurement of these methods is often limited to a few steps. An additional limitation of using such systems may also be in the fact that "natural" running steps cannot be simulated, e.g. when running on instrumented treadmills (Ammann et al., 2016).

In recent years, other temporal field measurement methods have been developed. These methods include e.g. Gobal Positioning System (GPS) embedded accelerometers and pressure sensitive insoles and footswitches. Buchheit and co-workers showed that random and systematic errors were of small to moderate amplitude in GPS-embedded accelerometers compared to criterion measurements obtained from an instrumented treadmill (Buchheit, Gray, & Morin, 2015). Studies have also shown that pressure sensitive insoles are a reliable and valid tool for measuring temporal characteristics compared to data from instrumented treadmills (Mann et al., 2014). Accelerometers are commonly found in GPS units worn by many team sport players around the world. Single inertial measurement units (IMU) mounted on the trunk have also shown to have the potential to provide reliable estimates of temporal parameters (Bergamini et al., 2012). Furthermore, optical measurement systems like Optojump (Microgate, Bolzano, Italy) have successfully been used by strength and conditioning coaches. However, this method has been shown to give less accurate, although reliable, measurements during running compared to IMU measurements, and seems therefore less valid for use in research (Ammann et al., 2016).

3.2 Sprint force-velocity profiling methods

Sprint performance can be described based on temporal characteristics, kinematics and kinetics. While t_c and t_f provides information on each step, a new method of force-velocity profiling provides information on the run as a whole. In recent years, force-velocity (F-v) and power-velocity (P-v) profiling of sprinting has evolved to be a useful tool to assess sprinting ability. The application of this method has the potential to optimize and individualize sprint training methodology. Samozino et al. (2016) proposed a simple method for determining the F-v and P-v relationships. The method requires only split times or instantaneous velocity measurements and anthropometric data, and is much easier to implement than other methods, such as instrumented treadmills or running tracks with force plates connected in series. These tools proved to be expensive and require in-depth technical knowledge of their implementation

therefore not suitable in field settings. The spatiotemporal data of a single sprint as proposed by Samozino et al. (2016) are easily obtained with photocells or by radar technology along the running track.

Until recently, the measurement of force and power properties in sprint running was a complicated task that required either a specific instrumented treadmill or a running track with several force plates in serial connection. However, the introduction of a new application (MySprintApp, FITProject, Spain) (Romero-Franco et al., 2017) provided sprinting profiles at a reasonable cost, simply by filming the athlete running and marking certain frames during the sprint, based on an external reference frame of 5 m intervals. This method allows the implementation and consistent monitoring of sprinting related mechanical properties (Mendiguchia et al., 2016).

Another method has been introduced to assess the athlete's ability to produce power (Jaric, 2015). It consists of performing repeated trials with progressively increasing load and provides data with decreasing velocity (peak velocity attained each trial) and associated increasing force production, resulting in a linear F-v relationship. From this, power can be computed as the integral of force and velocity (Cross, 2016). However, this method requires multiple pieces of equipment (videography or radar and sleds of different weights) thus making its implementation less suitable.

Force-velocity and P-v profiles provide information on sprint performance (i.e. sprint time and/or velocity) and the mechanical effectiveness of force application (Morin, Edouard, & Samozino, 2011). These F-v and P-v profiles are determined by the net horizontal impulse of each step. A description of temporal characteristics together with these profiles provide additional information about sprinting performance. The ability to obtain these profiles in combination with temporal characteristics within one system would enhance the ability to evaluate individual athletes, determine if their training should be force or speed specific, and detect differences in mechanical sprint properties between injured and non-injured athletes. Furthermore, it could possibly assist injury surveillance, as well as prevention processes and facilitate a more effective return to play strategy (Mendiguchia et al., 2016). Mendiguchia et al. (2016) speculated that a fatigue-induced decrease in V_0 and effectiveness of force application led to a dramatic increase in force output at the beginning of the sprint (F_{H0}). To maintain maximal velocity, an increase in force was needed. This increase in power put an unusually high stress on the hamstring muscle that resulted in injury (Mendiguchia et al., 2016; Schache, Dorn, Blanch, Brown, & Pandy, 2012). The ability to monitor

fatigue with force profiling could possibly prevent injury and give information that could assist in rehabilitation and return to play strategies (Mendiguchia et al., 2016).

3.3 Application of temporal characteristics-calculations and assessments

Temporal characteristic measurements which describe the different properties of human performance can be used to calculate leg stiffness, impulse and to assess asymmetry. However, the effect of these variables on performance is not well studied mainly due to the complicated measurement methods needed. The possibility of measuring t_c, subsequent calculation and easier access to the aforementioned variables will make advanced information more available and easier to study.

3.3.1 Leg stiffness

In the spring-mass models widely used to describe and study the mechanics of human running gait, the musculo-skeletal structures of the legs alternately store and return elastic energy, much like a spring (Alexander, 1988; Dalleau, Belli, Bourdin, & Lacour, 1998; Farley & Gonzalez, 1996). Leg stiffness (K_{leg}) is a key mechanical parameter derived from these models and is defined as the ratio between the maximal force applied to the leg spring and the maximum leg compression (i.e. the maximum deformation as it is exposed to force) (Morin et al., 2007). The spring mass model describes the body as a point of mass and the leg in contact with the ground during running as a spring (leg spring). When applied with force from the body, the spring will compress until it reaches the middle of the stance phase. The ratio between the amount of compression in the leg spring and the amount of force applied to it defines the stiffness of the leg spring (Farley & Gonzalez, 1996). Moreover, vertical stiffness (K_{vert}) is defined as the ratio of maximal force to the vertical displacement of the center of mass (CoM) as it reaches its lowest point, i.e., the middle of the stance phase. In short, vertical stiffness is a term used to describe the vertical motion of the CoM during ground contact (Farley & Gonzalez, 1996; Morin et al., 2005).

Changes in K_{leg} are mainly related to changes in t_c. Morin et al. (2007) claims that 90-96% of the variation in K_{leg} can be explained by variation in t_c and that step frequency may be an indirect factor through its effect on t_c (Morin et al., 2007). It has been established that at moderate velocities, K_{vert} increases while leg stiffness remains

constant (Brughelli & Cronin, 2008). However, it is unclear how leg stiffness is affected when velocity increases (Brughelli & Cronin, 2008). Taylor & Beneke (2012) compared K_{leg} of three world class sprinters and showed that K_{leg} for two of them were 1.6 and 1.5 times greater respectively, compared to slower sprinters (Hobara et al., 2010; Morin, Jeannin, Chevallier, & Belli, 2006). Greater vertical and leg stiffness helps resist the collapse of the body during contact and enhances force production during push off resulting in increased step frequency (Brughelli & Cronin, 2008). In contrast, the fastest sprinter had a lower step frequency, K_{leg} and K_{vert} and increased change in leg length (ΔL) and the maximal downward displacement of the CoM (Δy_c). These differences suggest a higher compliance, facilitating increased storage and utilization of elastic energy during the stretch shortening cycle (Brughelli and Cronin 2008). The increased t_c and lower step frequency allows an increase in impulse and distance travelled during contact (Beneke, Taylor, & Leithäuser, 2011).

Morin et al. (2005) proposed a method for calculating K_{leg} using t_c, t_f, velocity, body mass and length of the leg. Validation of this method showed low difference (0.12%-6%) between the force-platform and the model values. It was tested during a wide range of velocities (3.33 to 6.67 $m \cdot s^{-1}$ for the treadmill and 4 $m \cdot s^{-1}$ to maximal velocity on the force platform) with both physical education students experienced in treadmill running and elite middle-distance runners.

3.3.2 Impulse

Acceleration of the body is a key factor for determining performance in many sports such as soccer, rugby and American football (Faude, Koch, & Meyer, 2012; Robbins & Young, 2012), especially in sprint events. The acceleration phase (i.e. from the standing start to maximal speed) is directly related to sprint performance (Delecluse, 1997). Forward acceleration is related to the amount of net horizontal force and *impulse* applied and returned to the ground through the ground reaction force (GRF) impulse (Hunter, Marshall, & McNair, 2005; Kawamori, Nosaka, & Newton, 2013; Morin et al., 2015). The main determinants of motion in the sagittal plane are the vertical (F_V) and horizontal (F_H) force components and their corresponding impulses. Studies have shown that F_V production is related to the ability to achieve high maximal running speeds (Weyand, Sandell, Prime, & Bundle, 2010; Weyand, Sternlight, Bellizzi, & Wright,

2000) and that F_H is a clear determinant of acceleration and thus the 100m performance (Kugler & Janshen, 2010, Morin et al. 2011, Rabita et al. 2015). Vertical impulse has been shown to be either poorly or not significantly correlated with acceleration (Hunter et al., 2005; Kawamori et al., 2013). Morin et al. (2015) confirmed these results and showed that faster runners are those producing higher amount of horizontal net impulse per unit body mass. Furthermore, they showed that faster sprinters produce higher propulsive horizontal impulses, but not necessarily lower horizontal braking impulses.

3.3.3 Asymmetry

The effect of inter-limb asymmetry on performance in sprint running is unclear. Inter-limb asymmetry has been observed in sprinters at different performance levels. Haugen, Danielsen, McGhie, Sandbakk, and Ettema (2018) showed a difference of 0.6% between the "fastest" and "slowest" leg for athletes with a mean maximal velocity greater than 10 $m.s^{-1}$. This result is somewhat higher than the 0.3% reported for males with mean maximal velocity of 9.05 $m.s^{-1}$ (Exell, Irwin, Gittoes, & Kerwin, 2016) and considerably lower than the 4% for physical active males (Girard, Brocherie, Morin, & Millet, 2017). A difference in leg velocity of 0.6% might seem insignificant, but it represents nearly half of the average performance progression observed from the age of 18 to peak performance reached in the mid-20s for Norwegian competitive sprinters (Haugen, Tønnessen, & Seiler, 2015). For step length and step frequency, asymmetries between 1 and 4% have been measured (Exell et al., 2016; Girard, Brocherie, Morin, & Millet, 2017; Haugen et al., 2018) These studies show only small to no significant association between asymmetry and sprint performance.

From a clinical perspective, sprint asymmetry is used to assess the effectiveness of rehabilitation programs and to establish baseline values which can be used as pre-injury reference (Haugen et al., 2018). There are several studies that suggest a greater risk for injury in the weaker limb when strength and power imbalances are above 10% (Croisier, Forthomme, Namurois, Vanderthommen, & Crielaard, 2002; Sugiura, Saito, Sakuraba, Sakuma, & Suzuki, 2008).The information on imbalances in sprint specific movement patterns in relation to injury risk is limited (Haugen et al., 2018). However, Schache, Wrigley, Baker, and Pandy (2009) looked at inter-limb differences for several biomechanical parameters in different trials before the occurrence of a hamstring injury

in a sprinting athlete. This study showed imbalances between legs in vertical GRF peak and loading rate (7%, 73%), peak hip power generation (30%) and peak hamstring muscle-tendon unit length (11.7ms) of the long head of the biceps femoris. Information on limb asymmetry in resisted running with different loads in different populations is inexistent.

The ability to directly measure temporal characteristics during sprint and training with loads gives great opportunity to study these leg asymmetries. Although the role of inter-limb asymmetry as a cause of injury is not well known, the implementation of a system that provides valid data for monitoring and discovering patterns, is of great interest to the athlete and coach. Furthermore, this information can also be used to evaluate rehabilitation programs and help in the return-to-play decision making.

4. Material and Methods

4.1 Subjects

Seven sports science students with little to no experience in sprint running and one sprinter competing on national and international level. Only the sprinter was familiar with resisted sprint running. The subjects were asked to refrain from heavy strength training one day prior to testing.

Table 1: *Shows anthropometrics (sex, weight(kg), height (cm) and age (years(yrs))) for the subjects, and number of subjects for each sex. Data is shown as average with standard deviation.*

Sex(n)	Height (cm)	Weight (kg)	Age (yrs)
Male (6)	182.2 ± 4.2	81.7 ± 6.9	26.8 ± 1.7
Female (2)	164.5 ± 4.5	67.0 ± 3	23.5 ± 0.5

All participants were informed about the test protocols and gave their written consent before taking part in the study. The study was conducted according to the Declaration of Helsinki on ethical principles for medical research in human subjects, reviewed and approved by the Local Ethics committee of the Norwegian School of Sport Sciences (NSSS) and the Norwegian Centre for Research Data (NCRD) prior to the start of the study.

4.2 Measurement equipment

4.2.1. Criterion instrument

To accurately measure contact and flight time we used thin film force sensitive resistors (FSR; Biosignalsplux, Lisbon, Portugal) placed under the insole of each shoe. The sensors had a range of up to 150 Kg, a response time of <1.2 ms and a repeatability error of ±2.5%. The sensors were taped on the insole approximately underneath the 1st metatarsophalangeal joint. To find the point on to which the sensor was to be taped,

each subject stood on the insoles on the floor, and the point of contact was determined by palpating the pressure of the ball of the foot. The FSR sensors cable was taped to the leg with appropriate slack at each joint to keep the acquisition system from disturbing the running movement. If the participant wore long tights, the cable was placed on the inside of the tights and no tape was used, as shown in the picture below (Figure 2). The FSR wire was connected to the Bioplux wireless hub which was placed on the side of the hip on the lining of the subject's attire. FSR data were collected through the OpenSignals (r)evolution software (Biosignalsplux, Lisbon, Portugal) at a sampling rate of 1000 Hz. Due to the limited range of the Bluetooth connection (up to ~10m) when using online recording of the data, recording was scheduled through the OpenSignals software before each run. Each recording lasted one minute and was stored on the memory of the wireless hub. After the testing session was done, the recorded data was uploaded to a personal computer.

Figure 2: *Pictures show how the FSR sensors were taped on the insole and the placement of the Bioplux wireless hub on the clothing.*

4.2.2. 1080 Motion Sprint

Figure 3: *1080 Sprint, device used during testing.*

Sprint kinetics and kinematics were measured with the 1080 Sprint (1080 Motion, Lidingö, Sweden) which is a portable resistance and testing device used for various sports, particularly in running, skating, and swimming. Force data is calculated from the voltage in the electric motor, while velocity is calculated from time and distance. Velocity is then derived to calculate the acceleration data. A 1.5 Kw servo motor (2000 RPM OMRON G5 Series Motor, OMRON Corporation, Kyoto, Japan) provides continuous resistance (1-15 Kg) and maximum resistance of 30 and 45 Kg over 10 and 3 seconds respectively. A composite fiber cord is attached to the motor and wrapped around a spool, it can extend up to 90 meters. The cord was attached to a belt around the participants hips (1080 Motion, Lidingö, Sweden). The resistance is controlled by the Quantum computer application (1080motion webapp) (1080 Motion, Lidingö, Sweden), which also records all kinetic data of the sprint trials with a frequency of 333 Hz. The device was placed on the ground during testing (Figure 3).

4.3. Measurement Protocol

The subjects were tested twice in the sports hall of NSSS. Each test lasted for approximately two hours. All testing was performed in preferred training clothes and running shoes. There was no standardized time on the day of testing due to availability of the testing facilities. Both test days started with a *standardized warm up* consisting of 10 minutes easy running, four sprint-specific warm up exercises (walking lunges, punter kicks, B-skips, stiff ankle skips) with ten repetitions for each leg, and dynamic

stretching followed by four 30m runs with increasing speed (up to 95% of max). The subjects performed two 30 m runs with increasing speed before starting actual testing due to the time pause to insert the sensors in the shoes.

Testing consisted of two sets of five, 30 m runs with increasing resistances (1, 3, 6, 9 and 12 Kg). Five minutes rest between each run. During the first set of runs the resistance was set to isotonic. This setting makes the load constant throughout the entire run. During the second set of runs the resistance setting was set to "no flying weight". With this setting the subject must overcome the inertia of the resistance as he/she is accelerating. When the inertia has been overcome, the resistance becomes isotonic for the remaining duration of the run. This means that the load was heavier at the beginning, similar to the feeling when using sleds. The subjects wore a belt around the hips which was attached to the 1080 sprint cable. Each run started from the same spot with a standing start. The subjects stood with their preferred foot first. For each run, the acquisition of FSR data was programmed to record continuously for one minute. One minute before starting each test, the participant was attached to the 1080 Sprint cable with a belt located at the hips. When the FSR recording started, the 1080 sprint recording was started manually, and the participant was told to run as soon as ready. When the runner passed the 30 m mark, the 1080 Sprint recording was stopped manually.

4.4 Data analysis

All data were analyzed using a custom-made MATLAB R2017b (The MathWorks, Inc., Natick, Massachusetts, USA) program (Appendix II).

1080 Sprint data: Since the recording sampling frequency fluctuated just above and below 333 Hz, it was necessary to resample the data after which the acceleration data was wavelet transformed by Morlet wavelets (MatLab wavelet toolbox, "cwt" function, "amor" as argument) (Figures 4 and 5). Transformations in which the wavelets with frequencies above 5Hz were omitted, were carried out using the MatLab wavelet toolbox ("icwt" function). The peak (top) and minimal (bottom) values of the acceleration signal were extracted and lowest values were used to calculate step time.

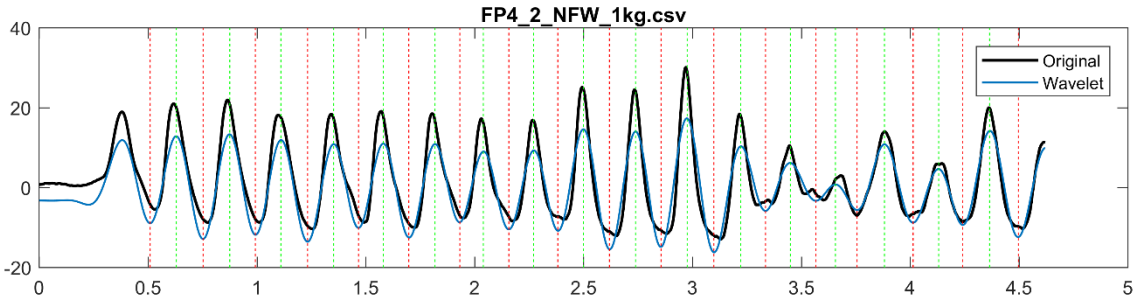

Figure 4: *Acceleration data ($m \cdot s^{-1}$) from 1080 Sprint (black) over time (s), with wavelet transformation as overlay (blue). Red dotted lines indicate lowest points, while green dotted lines indicate top points.*

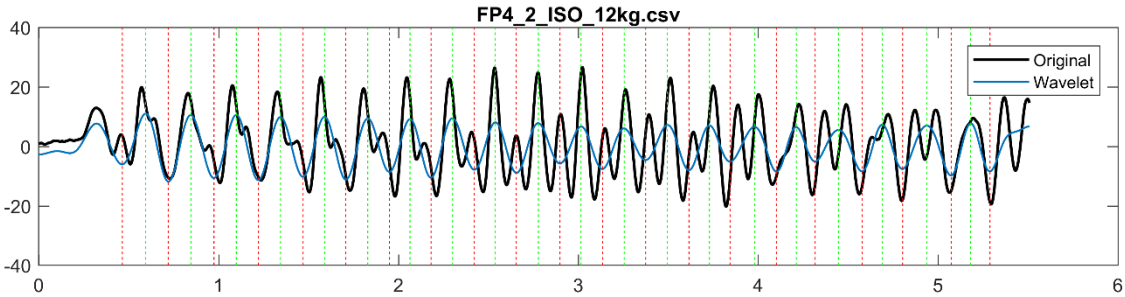

Figure 5: *Acceleration data (ms^{-1}) from 1080 Sprint (black) over time (s), with wavelet transformation as overlay (blue). Red dotted lines indicate lowest points, while green dotted lines indicate peak points. How "double peaks" in acceleration data affect the wavelet transformation.*

FSR data: The amplitude was normalized with its standard deviation due to variation between trials. A low-pass two-way Butterworth filter with 50 Hz cut-off frequency was used. Initial ground contact for one foot (toe-on) was defined as the instant when the FSR signal exceeded 3 times the median of the normalized FSR measurements. Toe-off (i.e. the last ground contact for one foot) was defined as the moment when FSR signal went below 3 times the median of the FSR measurement.

The data from the 1080 Sprint was synchronized with the FSR data by searching the data for the first acceleration above a certain threshold in the sprint data and the first peak above a certain threshold from the FSR sensors (Figure 6). Acceleration-, force-, and velocity-time data from the 1080 Sprint was then plotted in separate graphs with contact time measurements from FSR data for each step indicated with solid and dashed lines (Figures 7-9). Contact time was measured as the time from toe on to toe off (i.e. the time between the foot´s first and last contact with the ground).

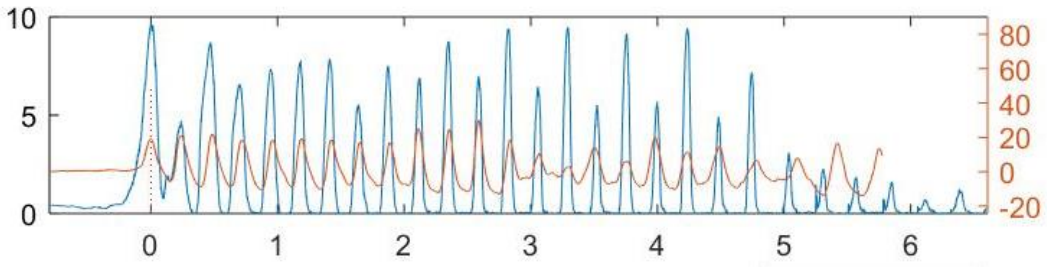

Figure 6: *Sprint acceleration data (orange, $m \cdot s^{-2}$) synchronized with FSR data (volt,V) over time(s).*

Step time (ST) was defined as the time from first point of ground contact of one foot, to the first point of ground contact for the second foot. In the FSR data this is the time from one toe-on to the next. Toe-on is in this thesis defined as first point of ground contact for one foot. Toe-off is defined as the last point of contact for the same foot. In the 1080 Sprint data, ST was defined as the difference in time from onset of positive acceleration of one oscillation to the onset of positive acceleration of the next.

4.5 Statistics

Bland and Altman plots were used to visualize systematic difference in step time predictions. The systematic difference represents the absolute difference between the measurement systems, and the random errors are calculated by the standard deviations of the difference between them, and then multiplied by 1.96. Together they form the 95% limits of agreement (Atkinson & Nevill, 1998; Bland & Altman, 1986). Pearson correlation coefficient (Pearson r) and R^2 was used to show correlation between the two methods while coefficient of variation (CV) showed the dispersion from the mean. Pearson r, R^2, CV's and Bland-Altman plots were calculated and plotted using Microsoft Excel 2016 (Microsoft Corporation, Redmond, USA).

5. Results

After visual inspection of the data it was decided that it would not be possible to approximate t_c. When inspecting the data, we looked for systematic patterns through the entire run like we see in figure 7. By systematic pattern we meant curves with cyclic behavior. Figure 7 is a graph with the pattern we looked for, typical for runs on low resistance (1 and 3kg)

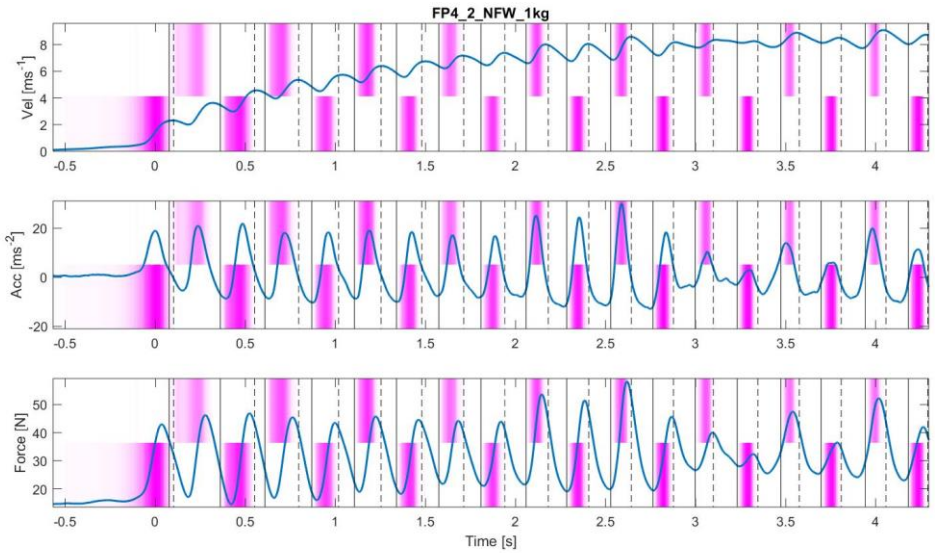

Figure 7: *Velocity (Vel (ms^{-1})), acceleration (Acc (ms^{-2})), Force (N) – data as a function of time (s) from 1080 Sprint compared with contact time data from FSR sensors (pink columns). The intensity of the color demonstrates the magnitude of the force measurement. Vertical lines represent toe-on(solid) and toe-off(dotted) determined by FSR-sensors. Resistance was set at 1 Kg.*

Figures 8 and 9 represent data from runs with examples of graphs were there was lack of a systematic cyclic pattern, i.e. where "double peaks" were observed from step 3 on. These "double peaks" occurred when applying the higher resistances (6, 9 and 12kg). The amplitude of these peaks was not consistent throughout the trials which made it impossible to determine systematic patterns in several runs across the different resistances and for the different subjects. Because of these problems and because of the high variation in the data, we decided to estimate ST instead of contact time. The onset of positive acceleration was defined as first point of contact as this seemed to be the most reliable throughout all runs. ST was therefore measured as the time from the first point of contact of one foot to the first point of contact of the other foot.

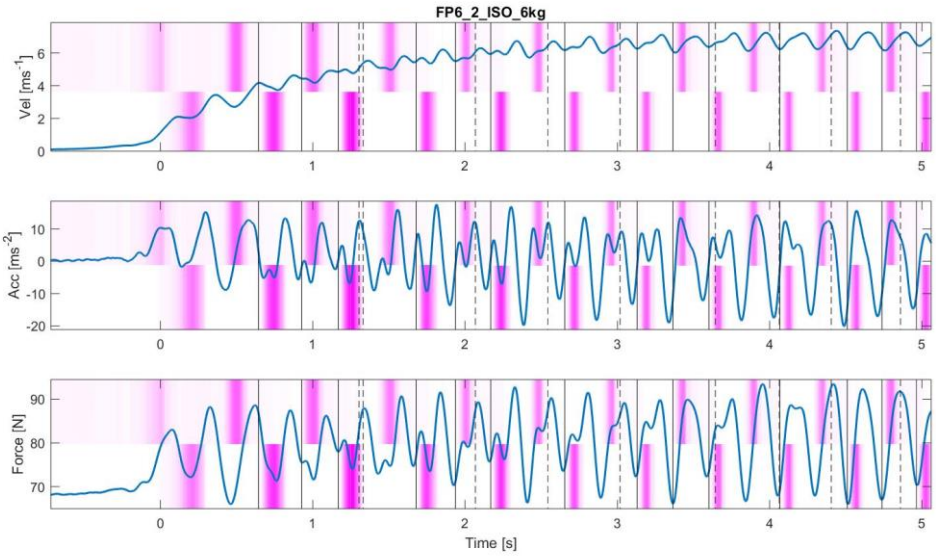

Figure 8: *Velocity (Vel (ms^{-1})), acceleration (Acc (ms^{-2})), Force (N) – data as a function of time (s) from 1080 Sprint compared with contact time data from FSR sensors (pink columns). The intensity of the color demonstrates the magnitude of the force measurement. Vertical lines represent toe-on(solid) and toe-off(dotted) determined by FSR-sensors. Resistance was set at 6 Kg. Example of a bad trial that made it impossible to approximate t_c.*

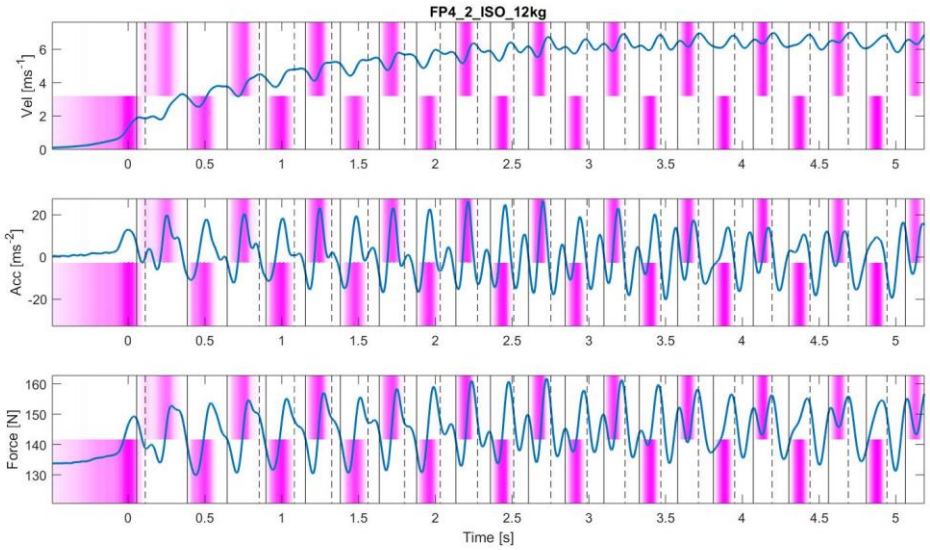

Figure 9: *Velocity (Vel (ms^{-1})), acceleration (Acc (ms^{-2})), Force (N) – data as a function of time (s) from 1080 Sprint compared with contact time data from FSR sensors (pink columns). The intensity of the color demonstrates the magnitude of the force measurement. Vertical lines represent toe-on(solid) and toe-off(dotted) determined by FSR-sensors. Resistance was set at 12 Kg. Example of a run with "double peaks" occurring.*

The three graphs in figure 7, 8 and 9 show velocity-, acceleration-, and force-data from the 1080 Sprint combined with T_c measured by the FSR sensors (pink columns). The solid lines represent the point of initial contact of one foot, while the following dashed line indicates the end of ground contact. The large pink area at the start is caused by the pressure on the sensor while the subject is standing in the starting position. The other pink areas represent foot ground contact. The intensity of the color indicates the amplitude of the FSR signal. Acceleration data oscillate with consistent amplitude during the first second, then the amplitude varies until the end of the trial. Force data also follows this pattern. Figure 9 displays the same as figure 8 but for a higher load (12kg). In this figure there are "double peaks" occurring around 1.5 seconds into the run. These double peaks continue throughout the trial.

Mean step time measured by the 1080 Sprint and FSR sensors was 248.48 ± 6.03 ms and 250.54 ± 5.52 ms, respectively (Table 2). For both methods, higher step time was registered with increasing resistance. Mean Pearson correlation coefficient was 0.7, mean R^2 was 0.5, while mean CV was 6.14 %.

Table 2: *Step time (ST) and coefficient of variation (CV) as a function of resistance and resistance mode. Values are means ± standard deviation (SD).*

Resistance	ST 1080sprint (ms)	ST FSR sensor (ms)	Pearson r/R^2	Coefficient of variation (CV, %)
ISO 1kg	239.35 ± 20.22	242.41 ± 17.96	0.67/0.45	6.41
ISO 3kg	242.29 ±17.04	243.98 ± 17.43	0.76/0.58	4.95
ISO 6kg	248.16 ±18.83	251.83 ± 19.17	0.68/0.46	6.26
ISO 9kg	249.60 ±21.26	252.83 ± 21.05	0.72/0.52	6.39
ISO 12kg	257.0 ± 22.81	257.68 ± 19.6	0.64/0.41	7.11
NFW 1kg	241.26 ±16.77	243.08 ± 15.69	0.70/0.49	5.30
NFW 3kg	245.89 ±17.84	248.82 ± 17.4	0.70/0.49	5.61
NFW 6kg	251.0 ± 21.86	252.62 ± 20.9	0.64/0.41	7.20
NFW 9kg	252.51 ± 23.83	253.50 ± 22.05	0.73/0.53	6.77
NFW 12kg	257.82 ± 23.35	258.72 ± 22.46	0.78/0.61	5.44

Legend: ISO = Isokinetic resistance; NFW = No flying weight resistance.

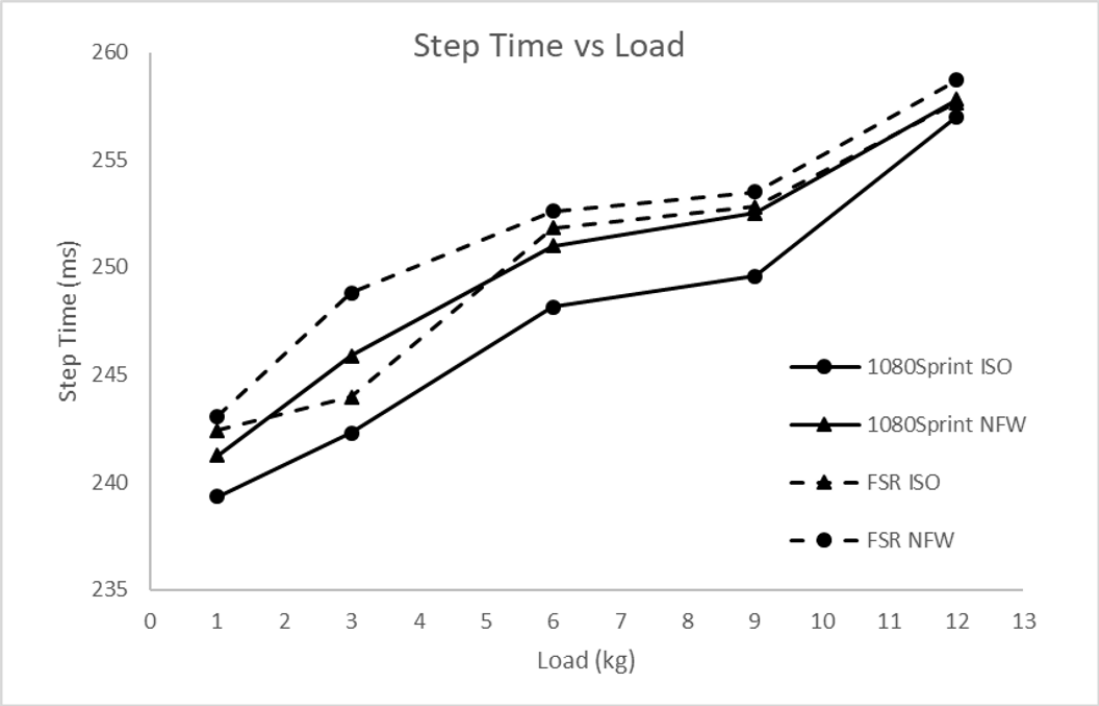

Figure 10: *Mean step time(ms) as a function of load(kg) for 1080Sprint and FSR. Dots and triangles represent loads used during trials. ISO = Isokinetic resistance; NFW = No flying weight resistance.*

Figure 10 illustrates the ST with increasing with load. A mean ST increase of 16 ms from 1 to 12kg for both methods and type of resistance.

The Bland-Altman plots showing the systematic differences and random errors are displayed in Figures 11 and 12. Each dot represents a measured ST for each of the subjects at the given load. The mean systematic difference between the two methods was 2.05 ms ± 1.08. The 95% confidence interval (CI) represent the magnitudes of random errors in relation to the systematic difference. The mean CI was +32.15 ms ± 3.98 and -28.03 ms ± 4.58. In all plots the data are clustered around 240-250 ms, with a small spread toward 300 ms. There are some outliers, but they lie so close to the 95% CI that they can be ignored.

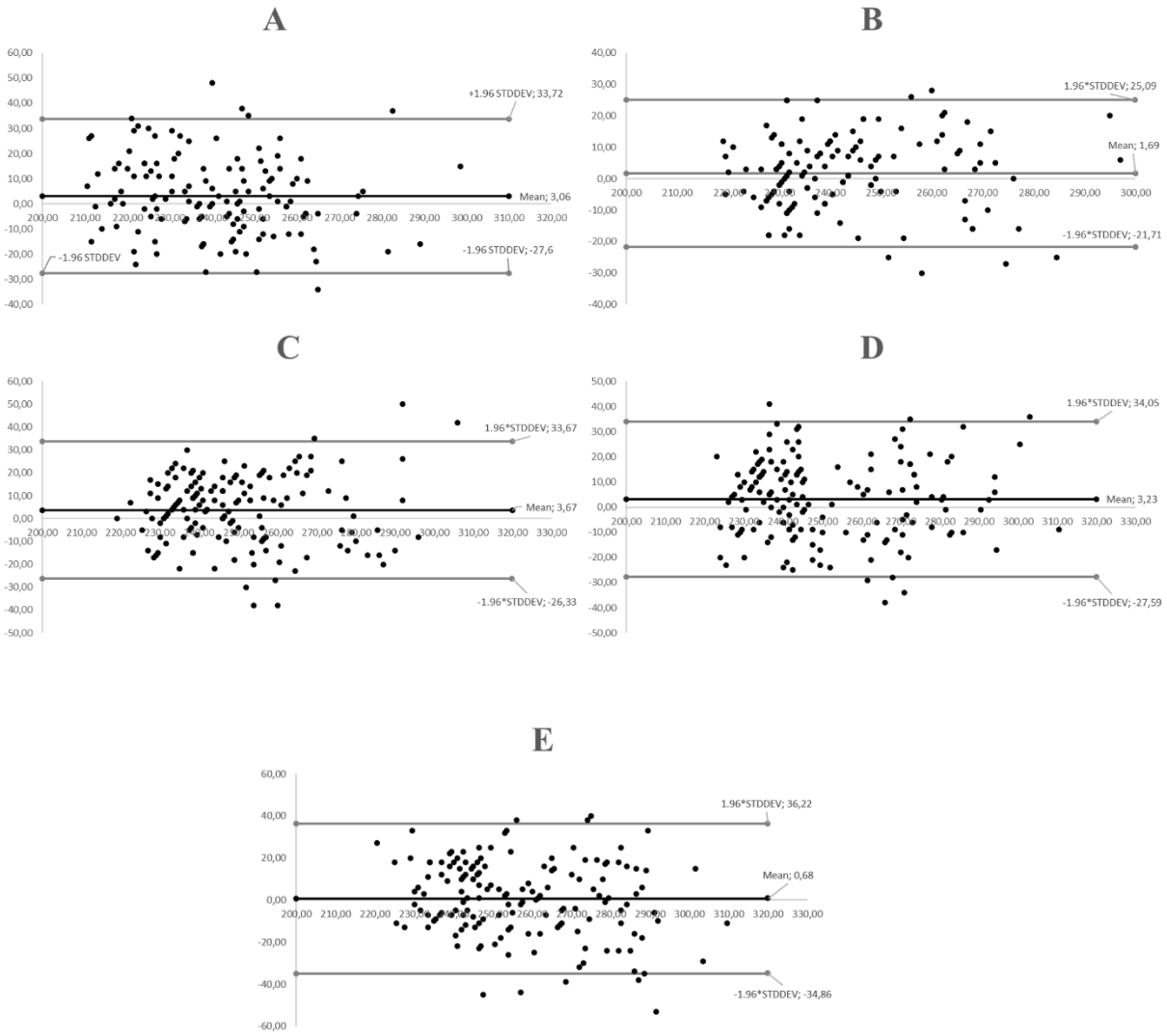

Figure 11: *Bland-Altman plots of the individual steptimes for all subjects during different loads with isotonic resistance (ISO). A: ISO 1kg, B: ISO 3kg, C: ISO 6kg, D: ISO 9kg, E: ISO 12kg. ISO = Isotonic resistance.*

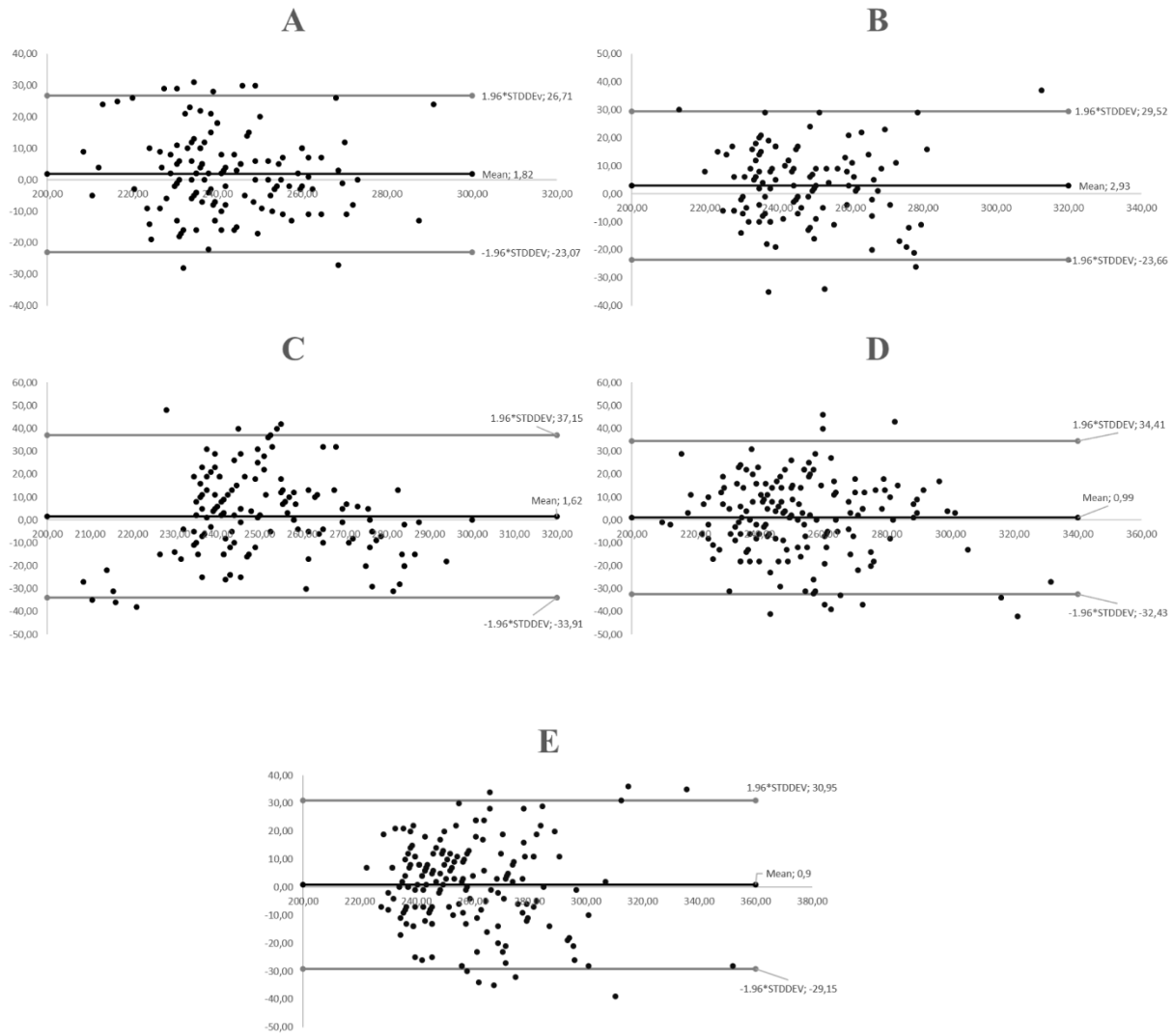

Figure 12: *Bland-Altman plots of the individual step times for all subjects during different loads with "no flying weight" resistance (NFW). A: NFW 1kg, B: NFW 3kg, C: NFW 6kg, D: NFW 9kg, E: NFW 12kg. NFW = No flying weight resistance.*

6. Discussion

This study sought to explore the possibility of measuring temporal characteristics from the oscillations in the horizontal velocity-, acceleration- or force-time curves obtained by the 1080 Sprint. Our main goal was to explore whether it was possible to validly estimate t_c from the oscillations in the curves of the device, in comparison to data obtained from FSR (criterion validity). The oscillations followed a pattern that according to the manufacturer could be used to specify toe on and toe off. However, when compared to the FSR data, the patterns were found to not be consistent and systematic enough to determine toe off. Some runs showed a pattern that could be used to set toe off, but not across different resistances and subjects to be regarded as useable to make reliable estimates for this purpose. This made it impossible to accurately measure t_c. Although we were not able to discover a pattern for toe-off, we used onset of positive acceleration as point of toe-on and measurement of step time.

Pressure insoles are regarded as valid and reliable and are often used to measure temporal characteristics of gait and running. Mann et al. (2014) demonstrated that pressure-sensitive insoles are extremely accurate in detecting the initial moment of contact (<3 ms average difference) compared to an instrumented treadmill. The limits of agreement in their study for t_c and t_f were larger (29 and 30 ms, respectively). The overall difference for the temporal parameters was 1.2%. The results obtained in our study are comparable to those produced by Mann et al. (2014).

Ammann et al. (2016) studied the accuracy of inertial sensors for measuring ground contact times during running. Inertial sensors or inertial measurement units (IMU) consist of accelerometers, magnetometers and gyroscopes that can be used to measure temporal characteristics of movement. Using high speed cameras as reference method, the systematic difference for the inertial sensors, mounted on the shoe, was -1.9 ms with a random error of 17±6.1 ms for all running speeds. Watari, Hettinga, Osis, and Ferber (2016) compared t_c during running, measured by a torso mounted accelerometer to kinetic data. They showed less than 6 ms mean difference for the top speeds (3.3 $m \cdot s^{-1}$ to 3.9 $m \cdot s^{-1}$) and very good agreement (CCC range 0.82-0.87) between the kinetic and accelerometer methods. Mounted on the shank, accelerometers can also measure t_c. Purcell, Channells, James, and Barrett (2006) compared shank-mounted accelerometer measurements with force plate measurements and presented mean error of 2 ± 3 ms and

1 ± 1 ms during running and sprinting respectively. The systematic differences of the inertial sensor methods are similar to the difference we found with the 1080 Sprint. However, the random error of shoe mounted IMU is smaller than for the 1080 Sprint (17 ± 6.1ms vs 30 ± 4.3 ms) (Ammann et al., 2016). These studies show that the placement of the IMU is of some importance to accuracy of the measurements, and it seems that IMU placed on the shoe lace is most accurate.

Optical devices, like e.g. Optojump (Microgate), presents another method used in field measurements. In the same study mentioned earlier (Ammann et al., 2016), an Optojump was also validated. The systematic difference for the Optojump was 25.7 ms with a random error of ± 26.1ms when compared to high speed camera measurements. This systematic difference was much larger than the other methods, while the random error was similar to the 1080 Sprint (Ammann et al., 2016). Glazier and Irwin (2001) concluded that the error (4.1 ± 23.1 mm) in stride length estimates, was insufficient. Although the variable measured was not the same as the one measured by Ammann et al. (2016), or in our study for that matter, they came to the same conclusion. Notwithstanding that the measurements are not valid for scientific use, both studies highlighted the potential of the Optojump as an effective field training tool for strength and conditioning professionals (Ammann et al., 2016; Glazier & Irwin, 2001).

The systematic difference of the 1080 Sprint (2.05 ms) was very small and close to what has been found when validating pressure insoles and IMU (Ammann et al., 2016; Mann et al., 2014). Limits of agreement around 30 ms are similar for pressure insoles and the 1080 Sprint, while IMU was smaller (17 ms). Inertial sensors seem to be the most accurate with the lowest limits of agreement. However, the difference in systematic error is minimal (2.05 ms vs -1.9 ms).

Although there was a difference in the type of resistance used during 50% of the runs, there does not seem to be a difference in data output from the two settings (ISO and NFW). This does not come as a surprise as the NFW setting is isotonic resistance (same as ISO setting) during large parts of the trial, except for the acceleration phase. It was reported by subjects that the weight felt heavier at the beginning of the run during NFW setting. This is caused the fact that the runner with this setting had to overcome the inertia of the resistance when starting. The resistance became isotonic after this and the end of each run felt the same regardless of resistance setting.

To provide resistance, the device is pulling the runner backwards at a constant speed (1.5 $m \cdot s^{-1}$). This could lead to a deceleration when the athlete is in the air and not pushing off the ground. While the athlete is in contact with the ground and applying horizontal force, the acceleration becomes positive. As we hypothesized, the onset of positive acceleration in the oscillations can be used as a reliable point of reference for toe-on during running. Regrettably, as mentioned above, the data produced were not reliable enough to determine a reference for toe-off (see Figures 8 and 9). In both graphs we saw "double peaks" during defined stance phases. When compared with Figure 7 we clearly see the challenge with reliability of some of the data when trying to determine patterns that can be used to approximate temporal characteristics. It was therefore not possible to estimate contact time. Only at low resistances (1 and 3 Kg) some of the data allowed us to determine points at which we could define start and end of each stance phase (Figure 7). However, the results were not reliable enough to make estimates with high enough confidence.

When the resistance increased, "double peaks" appeared in the acceleration data (figure 8 and 9). The origin of these are unknown, but we hypothesize that these peaks might be the result of the athlete adjusting to the resistance at initial contact, i.e. there is a slight deceleration before the body can apply the force needed to overcome the resistance. When the foot is in contact with the ground, a slight internal rotation may occur in the hips due to the pulling force of the cable. This rotation must be overcome by an increase in force production that may result in a small delay and creating the second peak. The "double peaks" could perhaps indicate an asymmetry between the legs. The amplitude of both peaks' changes during the run, the first peak is higher at the start of the run, the second peak is higher during the middle of the run, but the peaks even out towards the end of the run (figure 9). The reason for the changes in peak amplitude is not known, but we speculate that this may be due to measurement errors of the device. These measurement errors could be caused by slack in the cable as the runner gets further from the device. And/or by movement in the belt because of the increased movement in the cable. The adequacy of the motor might also be a source of error. The motors ability to regulate resistance and adjust to rapid changes in speed might affect the measurements. Small delays in regulation might lead to larger inaccuracies in calculations of force and derived acceleration.

6.1 Limitations

It may seem farfetched that it would be possible to measure temporal characteristics from a cable tethered to a hip belt. Limiting factors, such as the influence of the belt and cable may have interfered with the results. The belt used in the study is standard equipment with the 1080 Sprint. When running, the belt stretches, and the attachment point of the cable is moved away from the athlete. This may create a small delay in the pulling force of the cable and therefore originate an underestimation of acceleration and velocity. Perhaps it would have been better to use a stiffer and tighter belt that does not stretch or move as much during running.

Another limiting factor may be the cable and the increasing distance during the sprint. As the athlete gets further from the device the cable starts to move from side to side. The angel of the cable at the start of the run could also be a factor to consider. When the device is placed on the ground, a steep angel from the hip belt to the spool is created when the runner is taking starting position. How the angle and movement of the cable affect the measurements is not known and might be worth investigating.

Individual running pattern and variation of the anatomical structure of the front foot first in contact with the ground could lead to a larger variation in results depending on the placement of the sensors. In this study we used one FSR sensor on each foot. It could be argued that this is not enough. The sensors were positioned approximately on the first metatarsophalangeal joint (MTP joint). Oversupination resulting in ground contact of the 4^{th} and 5^{th} MTP joints prior to the 1^{st} MTP could have added to an underestimation of step times. Increasing the number of sensors or using pressure sensitive insoles with several sensors may prevent this observation.

6.2 Conclusion

This thesis studied the validity of temporal characteristics from acceleration-, force-, and velocity-time curves of the 1080 Sprint. Our results showed a systematic overestimation of ST of 2.05 ms in the 1080 Sprint when compared to FSR results. The determination of contact times was considered to be unreliable and should therefore not be used.

6.3 Conflict of interest

Co-supervisor Ola Eriksrud holds a position with 1080 Motion AB, Sweden. The author did not receive any commercial funding or salary of any kind that would influence the thesis.

7. References

Alexander, R. (1988). The spring in your step: the role of elastic mechanisms in human running. *Biomechanics XI-A.(Edited by G. de Groot, AP Hollander, PA Huijing, and GI van Ingen Schenau)*, 17-25.

Ammann, R., Taube, W., & Wyss, T. (2016). Accuracy of PARTwear inertial sensor and Optojump optical measurement system for measuring ground contact time during running. *The Journal of Strength & Conditioning Research, 30*(7), 2057-2063.

Atkinson, G., & Nevill, A. M. (1998). Statistical methods for assessing measurement error (reliability) in variables relevant to sports medicine. *Sports Medicine, 26*(4), 217-238.

Beneke, R., Taylor, M. J., & Leithäuser, R. M. (2011). The Fastest Men's 100 m Sprint Final-Stature and Step Rate were Cues for Success. *Medicine & Science in Sports & Exercise, 43*(5), 688.

Bergamini, E., Picerno, P., Pillet, H., Natta, F., Thoreux, P., & Camomilla, V. (2012). Estimation of temporal parameters during sprint running using a trunk-mounted inertial measurement unit. *Journal of biomechanics, 45*(6), 1123-1126.

BiosignalsPlux. FSR Sensor Datasheet. Retrieved from http://biosignalsplux.com/datasheets/FSR_Sensor_Datasheet.pdf

Bland, J. M., & Altman, D. G. (1986). Statistical methods for assessing agreement between two methods of clinical measurement. *The lancet, 327*(8476), 307-310.

Brughelli, M., & Cronin, J. (2008). Influence of Running Velocity on Vertical, Leg and Joint Stiffness. *Sports Medicine, 38*(8), 647-657. doi:10.2165/00007256-200838080-00003

Brughelli, M., Cronin, J., & Chaouachi, A. (2011). Effects of running velocity on running kinetics and kinematics. *The Journal of Strength & Conditioning Research, 25*(4), 933-939.

Buchheit, M., Gray, A., & Morin, J.-B. (2015). Assessing stride variables and vertical stiffness with GPS-embedded accelerometers: preliminary insights for the monitoring of neuromuscular fatigue on the field. *Journal of sports science & medicine, 14*(4), 698.

Bushnell, T., & Hunter, I. (2007). Differences in technique between sprinters and distance runners at equal and maximal speeds. *Sports biomechanics, 6*(3), 261-268.

Croisier, J.-L., Forthomme, B., Namurois, M.-H., Vanderthommen, M., & Crielaard, J.-M. (2002). Hamstring muscle strain recurrence and strength performance disorders. *The American journal of sports medicine, 30*(2), 199-203.

Cronin, J., Hansen, K., Kawamori, N., & McNair, P. (2008). Effects of weighted vests and sled towing on sprint kinematics. *Sports Biomech, 7*(2), 160-172. doi:10.1080/14763140701841381

Cross. (2016). *Force-velocity Profiling in Sled-resisted Sprint Running: Determining the Optimal Conditions for Maximizing Power.* Auckland University of Technology,

Dalleau, G., Belli, A., Bourdin, M., & Lacour, J. R. (1998). The spring-mass model and the energy cost of treadmill running. *European journal of applied physiology and occupational physiology, 77*(3), 257-263.

Debaere, S., Jonkers, I., & Delecluse, C. (2013). The contribution of step characteristics to sprint running performance in high-level male and female athletes. *The Journal of Strength & Conditioning Research, 27*(1), 116-124.

Delecluse, C. (1997). Influence of strength training on sprint running performance. *Sports Medicine, 24*(3), 147-156.

Delecluse, C. (1998). Influence of strength training on sprint running performance. *Occupational Health and Industrial Medicine, 1*(38), 44.

Di Michele, R., & Merni, F. (2014). The concurrent effects of strike pattern and ground-contact time on running economy. *Journal of Science and Medicine in Sport, 17*(4), 414-418.

Exell, T., Irwin, G., Gittoes, M., & Kerwin, D. (2016). Strength and performance asymmetry during maximal velocity sprint running. *Scand J Med Sci Sports*. doi:10.1111/sms.12759

Farley, C. T., & Gonzalez, O. (1996). Leg stiffness and stride frequency in human running. *Journal of biomechanics, 29*(2), 181-186.

Faude, O., Koch, T., & Meyer, T. (2012). Straight sprinting is the most frequent action in goal situations in professional football. *Journal of sports sciences, 30*(7), 625-631.

Girard, O., Brocherie, F., Morin, J. B., & Millet, G. P. (2017). Lower limb mechanical asymmetry during repeated treadmill sprints. *Hum Mov Sci, 52*, 203-214. doi:10.1016/j.humov.2017.02.008

Glazier, P., & Irwin, G. (2001). Validity of stride length estimates obtained from optojump.

Haugen, T., Danielsen, J., McGhie, D., Sandbakk, Ø., & Ettema, G. (2018). Kinematic stride cycle asymmetry is not associated with sprint performance and injury prevalence in athletic sprinters. *Scandinavian journal of medicine & science in sports, 28*(3), 1001-1008.

Haugen, T., Tønnessen, E., & Seiler, S. (2015). 9.58 and 10.49: Nearing the Citius End for 100 m? *International journal of sports physiology and performance, 10*(2), 269-272.

Hobara, H., Inoue, K., Gomi, K., Sakamoto, M., Muraoka, T., Iso, S., & Kanosue, K. (2010). Continuous change in spring-mass characteristics during a 400m sprint. *Journal of Science and Medicine in Sport, 13*(2), 256-261.

Hunter, J. P., Marshall, R. N., & McNair, P. J. (2004). Interaction of step length and step rate during sprint running. *Med Sci Sports Exerc, 36*(2), 261-271. doi:10.1249/01.MSS.0000113664.15777.53

Hunter, J. P., Marshall, R. N., & McNair, P. J. (2005). Relationships between ground reaction force impulse and kinematics of sprint-running acceleration. *Journal of applied biomechanics, 21*(1), 31-43.

Jaric, S. (2015). Force-velocity Relationship of Muscles Performing Multi-joint Maximum Performance Tasks. *Int J Sports Med, 36*(9), 699-704. doi:10.1055/s-0035-1547283

Kawamori, N., Nosaka, K., & Newton, R. U. (2013). Relationships between ground reaction impulse and sprint acceleration performance in team sport athletes. *The Journal of Strength & Conditioning Research, 27*(3), 568-573.

Mann, R., & Herman, J. (1985). Kinematic analysis of Olympic sprint performance: men's 200 meters. *International journal of sport biomechanics, 1*(2), 151-162.

Mann, R., Malisoux, L., Brunner, R., Gette, P., Urhausen, A., Statham, A., . . . Theisen, D. (2014). Reliability and validity of pressure and temporal parameters recorded using a pressure-sensitive insole during running. *Gait Posture, 39*(1), 455-459. doi:10.1016/j.gaitpost.2013.08.026

Mendiguchia, J., Edouard, P., Samozino, P., Brughelli, M., Cross, M., Ross, A., . . . Morin, J. B. (2016). Field monitoring of sprinting power-force-velocity profile before, during and after hamstring injury: two case reports. *J Sports Sci, 34*(6), 535-541. doi:10.1080/02640414.2015.1122207

Microgate, B., Italy. What is Optojump? Retrieved from http://www.optojump.com/What-is-Optojump.aspx

Morin, J. B., Dalleau, G., Kyröläinen, H., Jeannin, T., & Belli, A. (2005). A simple method for measuring stiffness during running. *Journal of applied biomechanics, 21*(2), 167-180.

Morin, J. B., Edouard, P., & Samozino, P. (2011). Technical ability of force application as a determinant factor of sprint performance. *Med Sci Sports Exerc, 43*(9), 1680-1688. doi:10.1249/MSS.0b013e318216ea37

Morin, J. B., Jeannin, T., Chevallier, B., & Belli, A. (2006). Spring-mass model characteristics during sprint running: correlation with performance and fatigue-induced changes. *Int J Sports Med, 27*(2), 158-165. doi:10.1055/s-2005-837569

Morin, J. B., Samozino, P., Zameziati, K., & Belli, A. (2007). Effects of altered stride frequency and contact time on leg-spring behavior in human running. *J Biomech, 40*(15), 3341-3348. doi:10.1016/j.jbiomech.2007.05.001

Morin, J. B., Slawinski, J., Dorel, S., de Villareal, E. S., Couturier, A., Samozino, P., . . . Rabita, G. (2015). Acceleration capability in elite sprinters and ground impulse: Push more, brake less? *J Biomech, 48*(12), 3149-3154. doi:10.1016/j.jbiomech.2015.07.009

MySprintApp, F., Spain. Retrieved from http://www.mysprintapp.com/

Nagahara, R., Mizutani, M., Matsuo, A., Kanehisa, H., & Fukunaga, T. (2018). Step-to-step spatiotemporal variables and ground reaction forces of intra-individual fastest sprinting in a single session. *Journal of sports sciences, 36*(12), 1392-1401.

Petrakos, G., Morin, J. B., & Egan, B. (2016). Resisted Sled Sprint Training to Improve Sprint Performance: A Systematic Review. *Sports Med, 46*(3), 381-400. doi:10.1007/s40279-015-0422-8

Purcell, B., Channells, J., James, D., & Barrett, R. (2006). *Use of accelerometers for detecting foot-ground contact time during running.* Paper presented at the BioMEMS and Nanotechnology II.

Rabita, G., Dorel, S., Slawinski, J., Saez-de-Villarreal, E., Couturier, A., Samozino, P., & Morin, J. B. (2015). Sprint mechanics in world-class athletes: a new insight into the limits of human locomotion. *Scand J Med Sci Sports, 25*(5), 583-594. doi:10.1111/sms.12389

Robbins, D. W., & Young, W. B. (2012). Positional relationships between various sprint and jump abilities in elite American football players. *The Journal of Strength & Conditioning Research, 26*(2), 388-397.

Romero-Franco, N., Jiménez-Reyes, P., Castaño-Zambudio, A., Capelo-Ramírez, F., Rodríguez-Juan, J. J., González-Hernández, J., . . . Balsalobre-Fernández, C. (2017). Sprint performance and mechanical outputs computed with an iPhone app: Comparison with existing reference methods. *European Journal of Sport Science, 17*(4), 386-392.

Samozino, P., Rabita, G., Dorel, S., Slawinski, J., Peyrot, N., Saez de Villarreal, E., & Morin, J. B. (2016). A simple method for measuring power, force, velocity properties, and mechanical effectiveness in sprint running. *Scand J Med Sci Sports, 26*(6), 648-658. doi:10.1111/sms.12490

Schache, A. G., Dorn, T. W., Blanch, P. D., Brown, N. A., & Pandy, M. G. (2012). Mechanics of the human hamstring muscles during sprinting. *Medicine & Science in Sports & Exercise, 44*(4), 647-658.

Schache, A. G., Wrigley, T. V., Baker, R., & Pandy, M. G. (2009). Biomechanical response to hamstring muscle strain injury. *Gait Posture, 29*(2), 332-338. doi:10.1016/j.gaitpost.2008.10.054

Sugiura, Y., Saito, T., Sakuraba, K., Sakuma, K., & Suzuki, E. (2008). Strength deficits identified with concentric action of the hip extensors and eccentric action of the hamstrings predispose to hamstring injury in elite sprinters. *J Orthop Sports Phys Ther, 38*(8), 457-464. doi:10.2519/jospt.2008.2575

Viitasalo, J. T., Luhtanen, P., Mononen, H. V., Norvapalo, K., Paavolainen, L., & Salonen, M. (1997). Photocell contact mat: a new instrument to measure contact and flight times in running. *Journal of applied biomechanics, 13*(2), 254-266.

Watari, R., Hettinga, B., Osis, S., & Ferber, R. (2016). Validation of a torso-mounted accelerometer for measures of vertical oscillation and ground contact time during treadmill running. *Journal of applied biomechanics, 32*(3), 306-310.

Weyand, P. G., Sandell, R. F., Prime, D. N., & Bundle, M. W. (2010). The biological limits to running speed are imposed from the ground up. *J Appl Physiol (1985), 108*(4), 950-961. doi:10.1152/japplphysiol.00947.2009

Weyand, P. G., Sternlight, D. B., Bellizzi, M. J., & Wright, S. (2000). Faster top running speeds are achieved with greater ground forces not more rapid leg movements. *Journal of applied physiology, 89*(5), 1991-1999.

List of tables

List of figures

Nomenclature

Δy_c	Center of mass displacement
ΔL	Change in leg length
CV	Coefficient of variation
CoM	Center of mass
F-v	Force-velocity
F_v	Vertical force
F_H	Horizontal force
FSR	Force Sensitive Resistor
GPS	Global positioning system
Hz	Hertz
IMU	Inertial Measurement Unit
ISO	Isotonic
Kg	Kilograms
K_{leg}	Leg stiffness
K_{vert}	Vertical stiffness
L-v	Load-velocity
mm	Millimeter

ms	Milliseconds
$m \cdot s^{-1}$	Meters per second
$m \cdot s^{-2}$	Meters per second per second
MTP joint	Metatarsophalangeal joint
NFW	No flying weight
P-v	Power-velocity
SL	Step length
ST	Step time
t_c	Contact time
t_f	Flight time

Appendix

I **Informed consent**

II **MatLab code**

Appendix I

Validering av power-, kraft-, hastighet-, og akselerasjon-tid kurver og temporale karakteristika som data fra 1080 Sprint

Bakgrunn og hensikt

Hensikten med denne studien er: 1) validere power-, kraft-, hastighet-, og akselerasjon-tid kurver og 2) definere kontakt- og svev-tid fra de samme kurvene i 1080 Sprint. Kraft-hastighet(F-v) og power-hastighet(P-v) profiler gir en generell beskrivelse av sprintløp. Utforming av slike kurver krever bruk av mellomtider fra ulike tidtakningsystemer (fotoceller, videografi eller laser) og implementering av tilleggsutstyr som sleder, om kurver for motstandsløp skal utformes. Systemer som måler tid, posisjon og kraft, samtidig som de gir motstand under løp, er nå tilgjengelige. Dette gir trenere, klinikere og forskere mulighet til å måle og kalkulere ulike profiler ved bruk av kun et system. Data fra løp med systemet viser sykliske mønster som kan skyldes individuelle steg, og kan dermed bli brukt til å studere temporale karakteristika, som kontakt og svevtid, i motstandsløp. Denne informasjonen gir mulighet til å studere asymmetri mellom bein og hvordan disse endres ved ulik motstand.

Per nå er det ingen måte å oppnå denne informasjonen uten bruk av en kombinasjon av ulike måleinstrumenter. Med evne til å kunne oppnå denne informasjonen med ett system, vil trenere og praktikanter få enkel tilgang til detaljert informasjon om individuelle utøveres løpsprofiler som kan bedre treningsarbeidet, testing, retur fra skade og skadeforebyggende arbeid. Dette gjelder ikke bare friidrett, men også lagidrett som for eksempel fotball, basketball og amerikansk fotball.

Hva innebærer studien?

Som deltager må du møte på Norges idrettshøgskole ved minimum to anledninger, for å løpe 10 motstandsløp. Måleinstrumenter som benyttes er 1080 sprint og trykksensitive sensorer som blir plassert i skoene. 1080 Sprint er en elektronisk vinsj som kan gi

isokinetisk motstand opp til 15kg. Kompositt wiren vil være festet til deg med et belte som blir plassert rundt hoftene. Sensorene vil bli plassert under innersålen på de foretrukne løpeskoene.

Mulige ulemper og risiko

De maksimale vil oppleves anstrengende. Det er en risiko for å pådra seg skader, spesielt strekkskader og/eller overtråkk, i forbindelse med maksimal sprint. Risikoen er ikke høyere enn ved vanlig løp/sprint.

Hva skjer med prøvene og informasjonen om deg?

Resultatene og informasjonen som registreres om deg skal kun brukes slik som beskrevet i hensikten med studien. Alle opplysninger og resultater vil bli behandlet uten navn, fødselsnummer eller andre direkte gjenkjennende opplysninger.
Det vil ikke være mulig å identifisere deg i resultatene i studien når disse publiseres.

Frivillig deltakelse

Hvis du ønsker å delta, undertegner du samtykkeerklæringen. Du kan når som helst, uten å oppgi grunn, trekke ditt samtykke til å delta i studien. Hvis du ønsker å trekke deg, eller har spørsmål til studien, vennligst ta kontakt med Ola Røkke på epost: ola@roekke.net eller tlf. 464 28 244.

Samtykke til deltakelse i studien

Jeg er villig til å delta i studien

(signert av prosjektdeltaker, dato)

Jeg bekrefter å ha gitt informasjon om studien

(signert av testleder(e), dato)

Appendix II

MatLab code

Main program:

```
clear all
close all
%% define variables here (file paths, file name, )
fpath ='FILEPATH GOES HERE';
fname = {'FILENAMES GO HERE'}  ;

test = x; % number corresponding to the row number in "fname". test=2
gives second row of fname-matrix, i.e. the files from test 2

%% analysis section
% read data from sprint
[TimeSprint,Position,Speed,Acceleration,ForceSprint] =
Import1080Sprint_V2(fullfile(fpath,fname{test,1}));
% read data from plux
[timePlux,ForcePluxRaw] = importPlux(fullfile(fpath,fname{test,2}));
sf_plux = median(diff(timePlux)).^-1; % sample frequency [Hz]
scalePlux = 0.5e-3;% scale plux to some value close to sprint
acceleration measurements for easy plotting
ForcePluxRaw = ForcePluxRaw.*scalePlux;

% synchronize plux and sprint measurements. Resample to Plux sampling
% frequency.
[timeSync,sprintdataSync,FSRdataSync] =
ResampleAndSync_newFSR([TimeSprint,Position,Speed,Acceleration,ForceSp
rint],...
     [timePlux, ForcePluxRaw],'');
% find the start and stop of the run:
 [timeStart,timeVpeak,timeStop] =
findStartStopRun(sprintdataSync,timeSync);
 timerunning = [timeStart, timeStop];

% Find toe on and toe off
[toe_on_r,toe_off_r] =
GroundContact_newFSR(FSRdataSync(:,1),timeSync); %NBNB: check what
channel is what leg
[toe_on_l,toe_off_l] =
GroundContact_newFSR(FSRdataSync(:,2),timeSync); %NBNB: check what
channel is what leg


%% plot results

% new figure type:
figure('units','normalized','outerposition',[0.05 0.02 0.9 0.95])
h1 = subplot(3,1,1);
myYlim = [min(sprintdataSync(:,2))-1, max(sprintdataSync(:,2))+1];
imagesc(timeSync,myYlim,FSRdataSync'),hold on
set(gca,'Ydir','normal')
plot(timeSync,sprintdataSync(:,2),'LineWidth',1.5)
hold on
vline(toe_on_l,'k')
vline(toe_off_l,'k--')
vline(toe_on_r,'k')
```

```
vline(toe_off_r,'k--')
ylim([0 max(sprintdataSync(:,2))+0.5])
ylabel 'Vel [ms^{-1}]'
xlim(timerunning)
title(fname{test,1}(1:end-4),'interpreter','none')


h2 = subplot(3,1,2);
myYlim = [min(sprintdataSync(:,3))-1, max(sprintdataSync(:,3))+1];
imagesc(timeSync,myYlim,FSRdataSync'),hold on
set(gca,'Ydir','normal')
plot(timeSync,sprintdataSync(:,3),'LineWidth',1.5)
hold on
vline(toe_on_l,'k')
vline(toe_off_l,'k--')
vline(toe_on_r,'k')
vline(toe_off_r,'k--')
ylabel 'Acc [ms^{-2}]'
xlim(timerunning)
ylim(myYlim)

h3 = subplot(3,1,3);
myYlim = [min(sprintdataSync(timeSync>timeStart,4))-1,
max(sprintdataSync(timeSync>timeStart,4))+1];
imagesc(timeSync,myYlim,FSRdataSync'),hold on
set(gca,'Ydir','normal')
plot(timeSync,sprintdataSync(:,4),'LineWidth',1.5)
hold on
vline(toe_on_l,'k')
vline(toe_off_l,'k--')
vline(toe_on_r,'k')
vline(toe_off_r,'k--')
ylabel 'Force [N]'
xlabel 'Time [s]'
xlim(timerunning)
ylim(myYlim)

linkaxes([h1,h2,h3],'x')

colormap([ones(100,1) linspace(1,0,100)' ones(100,1)])


% old figures (remove if you like the new ones better)
% figure('Position',[50 50 1e3 400])
% plot(timeSync,FSRdataSync,'LineWidth',1.5)
% hold on
% vline(toe_on_l,'g--')
% vline(toe_off_l,'r--')
% vline(toe_on_r,'g-.')
% vline(toe_off_r,'r-.')
% xlabel 'Time [s]'
% ylabel 'FSR output [arb. units]'
% xlim(timerunning)
% title(fname{test,1}(end-11:end-4),'interpreter','none')
% % print(strcat('eventsfromFSR_',fname{test}(1:end-4)),'-dpng','-
r400') %prints figure to file
%
% figure('Position',[50 50 1e3 400])
% hold on
% plot(timeSync,sprintdataSync(:,3),'LineWidth',1.5)
% vline(toe_on_l,'g--')
```

```
% vline(toe_off_l,'r--')
% vline(toe_on_r,'g-.')
% vline(toe_off_r,'r-.')
% hline(0,'k-')
% xlabel 'Time [s]'
% ylabel 'Acc [ms^{-2}]'
% xlim(timerunning)
% title(strcat('Acceleration, ',fname{test,1}(end-11:end-
4)),'interpreter','none')
% % print(strcat('SprintAcc_',fname{test}(1:end-4)),'-dpng','-r400')%
prints figure to file
%
% figure('Position',[50 50 1e3 400])
% hold on
% plot(timeSync,sprintdataSync(:,2),'LineWidth',1.5)
% vline(toe_on_l,'g--')
% vline(toe_off_l,'r--')
% vline(toe_on_r,'g-.')
% vline(toe_off_r,'r-.')
% hline(0,'k-')
% xlabel 'Time [s]'
% ylabel 'Acc [ms^{-2}]'
% xlim(timerunning)
% title(strcat('Speed, ',fname{test,1}(end-11:end-
4)),'interpreter','none')
% print(strcat('SprintVel_',fname{test}(1:end-4)),'-dpng','-r400')

% figure('Position',[50 50 1e3 400])
% hold on
% plot(timeSync,sprintdataSync(:,4),'LineWidth',1.5)
% vline(timeSync(toe_on_l),'k--')
% vline(timeSync(toe_off_l),'r--')
% vline(timeSync(toe_on_r),'k-.')
% vline(timeSync(toe_off_r),'r-.')
% xlabel 'Time [s]'
% ylabel 'Force [N]'
% xlim(timerunning)
% title(strcat('Tension, ',fname{test,1}(end-11:end-
4)),'interpreter','none')
% print(strcat('SprintForce_',fname{test}(1:end-4)),'-dpng','-r400')
```

Functions:

Differentiate 2nd order:

```
function [dy,ddy] = differentiate_2nd_order(y,sf)
%input: matrix with signals, sample frequency.
%Output: First and second time derivative of the signal
%(first and last entry is set equal to its neighbor)+
% Uses a five point stencil approximation to the derivative:
%df/dt = (-f(+2h) + 8f(+1h) -8f(-2h) + f(-h))/12h

[n,m] = size(y);
if n<m
    y=y';
    temp=n;
    n=m;
    m=temp;
end
```

```
dt = 1/sf;

%pad signal, 2. order Taylor expansion:
dy_start =(y(2,:)-y(1,:))/dt;
ddy_start =(y(3,:)-2.*y(2,:)+y(1,:))/dt^2;
dy_stopp =(y(end,:)-y(end-1,:))/dt;
ddy_stopp =(y(end,:)-2.*y(end-1,:)+y(end-2,:))/dt^2;

%size(y)
y = vertcat(y(1,:)-dy_start.*(2*dt)-.5.*ddy_start.*(2*dt).^2,...
   y(1,:)-dy_start.*(Rodriguez et al.)-.5.*ddy_start.*(Rodriguez et
al.).^2,...
   y,...
   y(end,:)+dy_stopp.*(Rodriguez et al.)+.5.*ddy_stopp.*(Rodriguez et
al.).^2,...
   y(end,:)+dy_stopp.*(2*dt)+.5.*ddy_stopp.*(2*dt).^2);
%plot(y)

%[n,m] = size(y)
dy = nan(size(y));
ddy = nan(size(y));
n=length(y);

for i=3:n-2
    dy(i,:) = -y(i+2,:) + 8*y(i+1,:) - 8*y(i-1,:) + y(i-2,:);
    ddy(i,:) = -y(i+2,:) + 16*y(i+1,:) -30*y(i,:) +16*y(i-1,:) - y(i-
2,:);
end


% dy(1:2,:) = repmat(dy(3,:),2,1);
% dy(n-1:n,:) = repmat(dy(n-2,:),2,1);
dy = dy./(12*dt);
%
% for i=3:n-2
%     ddy(i,:) = -dy(i+2,:) + 8*dy(i+1,:) - 8*dy(i-1,:) + dy(i-2,:);
% end
ddy = ddy./(12*dt.^2);

%remove padding
dy = dy(3:n-2,:);
ddy = ddy(3:n-2,:);


end
```

Filter_butter2bidir:

```
function [filtered_data] = filter_butter2bidir(raw_data,fc,fs,type)
% Function  filter_butter2bidir creates a biderectional 2. order
butterworth filter (effectively 4. order
% due to the two passes), and filters the input data.
% input: raw data (filtering along each column), cutoff freq, sampling
% freq, type ['highpass', 'lowpass', 'bandstop', 'bandpass']
```

```
% output: filtered data, same size as raw data

N=2; %filter order
%fs = 1e3; % [Hz] samplerate
type = lower(type);
if (strcmp(type,'highpass')||strcmp(type,'high'))
    type = 'high';
elseif (strcmp(type,'lowpass')||strcmp(type,'low'))
    type = 'low';
elseif (strcmp(type,'bandstop'))
    type = 'stop';
elseif (strcmp(type,'bandpass'))
    type = 'bandpass';
else
    disp('Feil filtertype: bruk highpass, lowpass, bandpass, eller
notch');
end

Wn = 2*fc/fs; %normalisert cutoff
[b,a]=butter(N,Wn,type);
filtered_data = filtfilt(b,a,raw_data);

end
```

Find_startstoprun:

```
function [tstart,tpeak,tstop] = findStartStopRun(sprintarray,t)
%FINDSTARTSTOPRUN Summary of this function goes here
%   Detailed explanation goes here

v_stop_rel = -0.5; % stop when speed is 0.5m/s less than peak speed
v_start_threshold = 0.1; % start when speed is greater than this
threshold

samplefreq = median(diff(t)).^-1;
v_filt = filter_butter2bidir(sprintarray(:,end-2),1,samplefreq,'low');
[vpeak,peakind] = max(v_filt);

tpeak = t(peakind);
v_filt(1:peakind-1) = inf; % trick to allow next command to succeed
tstop = t(find(v_filt<vpeak-v_stop_rel,1));
tstart = t(find(sprintarray(1:peakind,end-2)<v_start_threshold));
tstart = tstart(end);


end
```

Groundcontact:

```
function [t_on,t_off] = GroundContact_newFSR(signal,time)
```

```
%GROUNDCONTACT_NEWFSR Summary of this function goes here
%   Detailed explanation goes here

cutoff_FSRdata = 15; % filter FSR-measurements with low pass filter
prior to differentiation
normforcethresh = 0.1;
sf_plux = 1e3; %[Hz]

signal = signal./std(BiosignalsPlux);
signal_filt =
filter_butter2bidir(signal,cutoff_FSRdata,sf_plux,'low');
[dforce,ddforce] = differentiate_2nd_order(signal_filt,sf_plux);

ddforce = ddforce./std(ddforce);
dforce = dforce./std(dforce);

[~,myEvents] = findpeaks(ddforce,'minpeakprominence',3);
t_on = [];
t_off = [];
for i=1:length(myEvents)
    if dforce(myEvents(i))>0 % t_on
        tmp = find(signal(1:myEvents(i))<normforcethresh,1,'last');
        t_on = cat(1,t_on,time(tmp));
    else
        tmp = find(signal(myEvents(i):end)<normforcethresh,1,'first')
+ myEvents(i)-1;
        t_off = cat(1,t_off,time(tmp));
    end
end

figure
plot(time,dforce)
hold on
plot(time,ddforce)
plot(time,[signal signal_filt])
hline(0,'k')
vline(t_on,'g--')
vline(t_off,'r--')

end
```

h_line:

```
function hhh=hline(y,in1,in2)
% function h=hline(y, linetype, label)
%
% Draws a horizontal line on the current axes at the location
specified by 'y'.  Optional arguments are
% 'linetype' (default is 'r:') and 'label', which applies a text label
to the graph near the line.  The
% label appears in the same color as the line.
%
% The line is held on the current axes, and after plotting the line,
the function returns the axes to
% its prior hold state.
%
% The HandleVisibility property of the line object is set to "off", so
not only does it not appear on
% legends, but it is not findable by using findobj.  Specifying an
output argument causes the function to
% return a handle to the line, so it can be manipulated or deleted.
Also, the HandleVisibility can be
% overridden by setting the root's ShowHiddenHandles property to on.
%
% h = hline(42,'g','The Answer')
%
% returns a handle to a green horizontal line on the current axes at
y=42, and creates a text object on
% the current axes, close to the line, which reads "The Answer".
%
% hline also supports vector inputs to draw multiple lines at once.
For example,
%
% hline([4 8 12],{'g','r','b'},{'l1','lab2','LABELC'})
%
% draws three lines with the appropriate labels and colors.
%
% By Brandon Kuczenski for Kensington Labs.
% brandon_kuczenski@kensingtonlabs.com
% 8 November 2001

if length(y)>1  % vector input
    for I=1:length(y)
        switch nargin
        case 1
            linetype='r:';
            label='';
        case 2
            if ~iscell(in1)
                in1={in1};
            end
            if I>length(in1)
                linetype=in1{end};
            else
                linetype=in1{I};
            end
            label='';
        case 3
```

```
            if ~iscell(in1)
                in1={in1};
            end
            if ~iscell(in2)
                in2={in2};
            end
            if I>length(in1)
                linetype=in1{end};
            else
                linetype=in1{I};
            end
            if I>length(in2)
                label=in2{end};
            else
                label=in2{I};
            end
        end
        h(I)=hline(y(I),linetype,label);
    end
else
    switch nargin
    case 1
        linetype='r:';
        label='';
    case 2
        linetype=in1;
        label='';
    case 3
        linetype=in1;
        label=in2;
    end



    g=ishold(gca);
    hold on

    x=get(gca,'xlim');
    h=plot(x,[y y],linetype);
    if ~isempty(label)
        yy=get(gca,'ylim');
        yrange=yy(2)-yy(1);
        yunit=(y-yy(1))/yrange;
        if yunit<0.2
            text(x(1)+0.02*(x(2)-
x(1)),y+0.02*yrange,label,'color',get(h,'color'))
        else
            text(x(1)+0.02*(x(2)-x(1)),y-
0.02*yrange,label,'color',get(h,'color'))
        end
    end

    if g==0
    hold off
    end
    set(h,'tag','hline','handlevisibility','off') % this last part is
so that it doesn't show up on legends
end % else

if nargout
```

```
    hhh=h;
end
```

import_1080sprint:

```
function [Time,Position,Speed,Acceleration,Force,Sampleduration] =
Import1080Sprint_V2(varargin)
%Import1080Sprint_v2 Import numeric data from a text file as column
vectors.
%   [Time,Position,Speed,Acceleration,Force,Sampleduration]
%   = IMPORTFILE(FILENAME) Reads data from text file FILENAME for the
%   default selection. If filename is not specified, the user is
prompted
%   to load one using uigetfile
%
% Example:
%   [Time,Position,Speed,Acceleration,Force,Sampleduration] =
Import1080Sprint_v2('Løp 1 3kg_1080 Sprint.csv');
%


if isempty(varargin)
    [filename,fpath] = uigetfile('*.csv','Select file to import');
    filename = fullfile(fpath,filename);
elseif length(varargin) == 1
    filename = varargin{1};
end

startRow = 2;
endRow = inf;
delimiter = {',',';'};
formatSpec =
'%*s%*s%*s%*s%*s%*s%*s%*s%*s%*s%*s%*s%s%s%s%s%s%s%[^\n\r]';

% Open the text file.
fileID = fopen(filename,'r');

% Read columns of data according to the format.
dataArray = textscan(fileID, formatSpec, endRow(1)-startRow(1)+1,
'Delimiter', delimiter, 'TextType', 'string', 'HeaderLines',
startRow(1)-1, 'ReturnOnError', false, 'EndOfLine', '\r\n');
for block=2:length(startRow)
    frewind(fileID);
    dataArrayBlock = textscan(fileID, formatSpec, endRow(block)-
startRow(block)+1, 'Delimiter', delimiter, 'TextType', 'string',
'HeaderLines', startRow(block)-1, 'ReturnOnError', false, 'EndOfLine',
'\r\n');
    for col=1:length(dataArray)
        dataArray{col} = [dataArray{col};dataArrayBlock{col}];
    end
end

%% Close the text file.
fclose(fileID);

%% Convert the contents of columns containing numeric text to numbers.
% Replace non-numeric text with NaN.
raw = repmat({''},length(dataArray{1}),length(dataArray)-1);
```

```
for col=1:length(dataArray)-1
    raw(1:length(dataArray{col}),col) = mat2cell(dataArray{col},
ones(length(dataArray{col}), 1));
end
numericData = NaN(size(dataArray{1},1),size(dataArray,2));

for col=[1,2,3,4,5]
    % Converts text in the input cell array to numbers. Replaced non-
numeric
    % text with NaN.
    rawData = dataArray{col};
    for row=1:size(rawData, 1)
        % Create a regular expression to detect and remove non-numeric
prefixes and
        % suffixes.
        regexstr = '(?<prefix>.*?)(?<numbers>([-
]*(\d+[\,]*)+[\.]{0,1}\d*[eEdD]{0,1}[-+]*\d*[i]{0,1})|([-
]*(\d+[\,]*)*[\.]{1,1}\d+[eEdD]{0,1}[-+]*\d*[i]{0,1}))(?<suffix>.*)';
        try
            result = regexp(rawData(row), regexstr, 'names');
            numbers = result.numbers;

            % Detected commas in non-thousand locations.
            invalidThousandsSeparator = false;
            if numbers.contains(',')
                thousandsRegExp = '^\d+?(\,\d{3})*\.{0,1}\d*$';
                if isempty(regexp(numbers, thousandsRegExp, 'once'))
                    numbers = NaN;
                    invalidThousandsSeparator = true;
                end
            end
            % Convert numeric text to numbers.
            if ~invalidThousandsSeparator
                numbers = textscan(char(strrep(numbers, ',', '')),
'%f');
                numericData(row, col) = numbers{1};
                raw{row, col} = numbers{1};
            end
        catch
            raw{row, col} = rawData{row};
        end
    end
end


%% Replace non-numeric cells with NaN
R = cellfun(@(x) ~isnumeric(x) && ~islogical(x),raw); % Find non-
numeric cells
raw(R) = {NaN}; % Replace non-numeric cells

%% Allocate imported array to column variable names
Sampleduration = cell2mat(raw(:, 5));
keepind = find(Sampleduration>0); % Discard samples with zero
duration.
Time = cumsum(Sampleduration(keepind));

Position = cell2mat(raw(keepind, 1));
Speed = cell2mat(raw(keepind, 2));
Acceleration = cell2mat(raw(keepind, 3));
Force = cell2mat(raw(keepind, 4));
```

```
%% linearly interpolate missing samples
interpmethod = 'linear';
Position = interpnans(Time,Position,interpmethod);
Speed = interpnans(Time,Speed,interpmethod);
Acceleration = interpnans(Time,Acceleration,interpmethod);
Force = interpnans(Time,Force,interpmethod);

    function array_out = interpnans(time,array_in,interpmethod)
        ind = find(~isnan(array_in)); % index of all samples that have
a numeric value
        array_out =
interp1(time(ind),array_in(ind),time,interpmethod);
    end

end
```

Import_Plux:

```
function [t,f] = importPlux(varargin)
%IMPORTPLUX Reads data exported from Opens signals.
%   Input: file name (with path if not in current directory) and
sampling
%   frequency of the Plux unit (normally 1000 Hz).
% output: time, numeric data in all columns that have data in them
(discarding zero-columns)


if isempty(varargin)
    [fname,fpath] = uigetfile('*.csv','Select file to import');
    fname = fullfile(fpath,fname);
elseif length(varargin) == 1
    fname = varargin{1};
end

% look for sampling frequency, should be hidden in the header
somewhere
fid = fopen(fname);
headerline = textscan(fid,'%s',2,'Delimiter','\n');
fclose(fid);
searchphrase = '"sampling rate": '; % sampling frequency is written to
the header after this phrase
lookhere = strfind(headerline{1}{2},searchphrase) +
length(searchphrase)-1;
endlook = strfind(headerline{1}{2}(lookhere:end),',') + lookhere-1;
samplefreq = str2double(headerline{1}{2}(lookhere:endlook));
if isnan(samplefreq)
    warning('Could not determine sampling frequency from open signals
header. Using default value og 1000 Hz')
    samplefreq = 1e3;
end


data = dlmread(fname,' ',3,0);
f = data(:,2:end);
nulcols = find(sum(f,1)==0 & std(f,[],1) ==0);
f(:,nulcols) = []; % discard columns that are zeros only
t = (0:length(f)-1)'./samplefreq;
```

```
if any(diff(data(:,1))>1)
    warning('Possibly missing sample(s). I will proceed, but check
file integrity')
end



end
```

Resample_and_Sync:

```
function [t_sync,sprintdata,FSRdata] =
ResampleAndSync_newFSR(SprintArray,FSRarray,method)
%RESAMPLEANDSYNC Reamples and and syncs sprint-data with FSR data. If
medhod='xcorr', the synchronization if done using
%cross correlations of FSR-output with Sprint acceleration. This
appears to be unreliable. Use method='' to skip cross correlations,
% this appears more robust. t=0 is then defined from the first large
% accelaration from sprint and the first large force peak from the
% FSR-sensors.

% input: Array of sprint data formatted as [time, data1, data2,...],
and
% similarly for FSR-data
% method: 'xcorr' for cross correlations (not robust), empty otherwise
% output: Arrays "sprintdata" and "FSRdata", time synchronized, and
the common
% time array for the two "t_sync"

autodetectstart = 1; % if 1: I will automatically attempt to detect
the start of the run. if zero the user is prompted to select this
manually

tsprint = SprintArray(:,1);
tFSR = FSRarray(:,1);
forceFSR = FSRarray(:,2:end);
dt = median(diff(tFSR));

figure
subplot(3,1,1)
if autodetectstart % attempt to detect start of race from signals
    [t0_FSR,i0_FSR] = getStartOfRaceFSR(tFSR,forceFSR);
    [t0_sprint,i0_sprint] =
getStartOfRaceSprint(tsprint,SprintArray(:,3),SprintArray(:,4));
    plot(tFSR-t0_FSR,sum(forceFSR,2)),hold on
    yyaxis right
    plot(tsprint-t0_sprint,SprintArray(:,4))
    legend('sum FSR','Sprint acc')
    vline(0)
else % select approximate location of sync signal in the data using
the ginput-function
    plot(tFSR,forceFSR);
    title 'Select start of race (FSR)'
    [t0_FSR,~] = ginput(1);
    [~,i0_FSR] = min(abs(t0_FSR-tFSR));
    forceFSR = forceFSR(:,FSRsyncChannel);

    plot(tsprint,SprintArray(:,end-1));
```

```
    title 'Select start of race (Sprint Acc)'
    [t0_sprint,~] = ginput(1);
    [~,i0_sprint] = min((tsprint-t0_sprint).^2);
end

t_off_approx = t0_FSR - t0_sprint
t_sync = tFSR-t0_FSR;

% interpolate sprint data to FSR rate
sprintdata = interp1(tsprint,SprintArray(:,2:end),tFSR-
t_off_approx,'linear');

if strcmp(method,'xcorr')
    % sync by cross correlations. Limit lags to +- 1 second.
    mywindow = round(1/dt);
    ind = (-mywindow:mywindow)' + round(i0_FSR);
    if ind(end)>length(forceFSR)
        indmax = find(ind>length(forceFSR),1);
        ind = ind(1:indmax-1);
    end
    % prepare signals to cross correlate
    corrsignal_sprint = sprintdata(ind,end-1);
    corrsignal_sprint(isnan(corrsignal_sprint)) = 0;
    corrsignal_plux = forceFSR(ind,:);
    corrsignal_plux =
corrsignal_plux./repmat(std(corrsignal_plux),[length(corrsignal_plux)
1]);
    corrsignal_plux = sum(corrsignal_plux,2);
    corrsignal_sprint = corrsignal_sprint-nanmean(corrsignal_sprint);
    corrsignal_plux = corrsignal_plux-mean(corrsignal_plux);

    % perform cross correlation
    [acor,lags] =
xcorr(corrsignal_sprint,corrsignal_plux,250,'unbiased');
    [~,tmp] = max(acor);
    maxlag = lags(tmp);

    % plot for validation
    subplot(3,1,2)
    plot(lags,acor),hold on
    title 'Result of sync procedure'
    ylabel 'Cross correlation'
    xlabel 'Lags [ms]'

    subplot(3,1,3)
    xax = (0:length(corrsignal_sprint)-1)';
    plot(xax,corrsignal_sprint)
    yyaxis right
    plot(xax+maxlag,corrsignal_plux)
    legend('Sprint acc','Plux force')
    title 'Result of sync procedure'
    ylabel 'Acc or force'
    xlabel 'Time [ms]'

    t_off_plux = -maxlag.*dt;
    % interpolate sprintdata according the the calculated sync offset
    sprintdata = interp1(t_sync,sprintdata,t_sync-
t_off_plux,'linear');
end

remrows = find(isnan(sprintdata(:,1)));
```

```
sprintdata(remrows,:) = [];
t_sync(remrows,:) = [];
FSRdata = FSRarray(:,2:end);
FSRdata(remrows,:) = [];



    function [t0,i0] = getStartOfRaceFSR(t,forceFSR)
        tmpsignal = forceFSR./repmat(std(forceFSR),[length(forceFSR)
1]);
        tmpsignal = sum(tmpsignal,2);
        [~,locs] = findpeaks(tmpsignal,'MinPeakProminence',3);
        i0 = locs(1);
        t0 = t(i0);
    end

    function [t0,i0] = getStartOfRaceSprint(t,speed,acc)
        vthresh = 1; %[m/s] speed defined as start
        % find last measurement with v<vthresh before v_max. This is
the start
        [~,i_max] = max(speed); % index of peak speed during the test
        i0 = find(speed(1:i_max)<vthresh,1,'last');
        [~,locs] = findpeaks(acc,'MinPeakHeight',5);
        [~,myLoc] = min((locs-i0).^2);
        i0 = locs(myLoc);
        t0 = t(i0);
    end



end
```